Analysis of chronic myeloid leukemia during deep molecular response by genomic PCR: a traffic light stratification model with impact on treatment-free remission

Katerina Machova Polakova[1,2], Hana Zizkova[1], Jan Zuna [3], Eliska Motlova[1], Lenka Hovorkova[3], Andrea Gottschalk[4], Ingmar Glauche[4], Jitka Koblihova[1], Pavla Pecherkova[1], Hana Klamova[1,5], Marketa Stastna Markova[1,5], Dana Srbova[1], Adela Benesova[1], Vaclava Polivkova[1], Tomas Jurcek[6], Daniela Zackova[7], Jiri Mayer[7], Thomas Ernst[8], Francois X. Mahon[9], Susanne Saussele[10], Ingo Roeder[4,11], Nicholas C.P. Cross[12], Andreas Hochhaus[8]

Running title: DNA PCR for a traffic light stratification of TFR

1 Institute of Hematology and Blood Transfusion, Prague, Czech Republic

2 Institute of Pathological Physiology, First Faculty of Medicine, Charles University, Prague, Czech Republic

3 CLIP, Dept. of Paediatric Haematology and Oncology, Second Faculty of Medicine, Charles University and University Hospital Motol, Prague, Czech Republic

4 Institute for Medical Informatics and Biometry (IMB), Carl Gustav Carus Faculty of Medicine, TU Dresden, Germany

5 Institute of Clinical and Experimental Hematology, First Faculty of Medicine, Charles University, Prague, Czech Republic

6 Center of Molecular Biology and Gene Therapy, Internal Hematology and Oncology Clinic, Faculty Hospital Brno and Faculty of Medicine, Masaryk University, Brno, Czech Republic

7 Internal Hematology and Oncology Clinic, Faculty Hospital Brno and Faculty of Medicine, Masaryk University, Brno, Czech Republic

8 Abteilung Hämatologie/Onkologie, Klinik für Innere Medizin II, University of Jena, Jena, Germany

9 Bergonié Cancer Institute, Inserm Unit 916, University of Bordeaux, Bordeaux, France

10 Department of Haematology and Oncology, University Hospital Mannheim, Heidelberg University, Mannheim, Germany

11 National Center for Tumor Diseases (NCT), Partner Site Dresden, Germany

12 Wessex Regional Genetics Laboratory, Salisbury NHS Foundation Trust, Salisbury and Faculty of Medicine, University of Southampton, Southampton, United Kingdom

Corresponding Author:

Katerina Machova Polakova

Institute of Hematology and Blood Transfusion

U Nemocnice 1

Praha 2

12800, Czech Republic

Phone: +420 221 977 305

E-Mail: katerina.machova@uhkt.cz

Abstract

This work investigated patient-specific genomic *BCR-ABL1* fusions as markers of measurable residual disease (MRD) in chronic myeloid leukemia, with a focus on relevance to treatment-free remission (TFR) after achievement of deep molecular response (DMR) on tyrosine kinase inhibitor (TKI) therapy. DNA and mRNA *BCR-ABL1* measurements by qPCR were compared in 2189 samples (129 patients) and by digital PCR in 1279 sample (62 patients). A high correlation was found at levels of disease above MR4, but there was a poor correlation for samples during DMR. A combination of DNA and RNA MRD measurements resulted in a better prediction of molecular relapse-free survival (MRFS) after TKI stop (n=17) or scheduled interruption (n=25). At 18 months after treatment cessation, patients with stopped or interrupted TKI therapy who were DNA negative/RNA negative during DMR maintenance (green group) had a molecular relapse-free survival (MRFS) of 80% and 100%, respectively, compared to those who were DNA positive/RNA negative (MRFS= 57% and 67%, respectively; yellow group) or DNA positive/RNA positive (MRFS=20% for both cohorts; red group). Thus, we propose a “traffic light” stratification as a TFR predictor based on DNA and mRNA *BCR-ABL1* measurements during DMR maintenance before TKI cessation.

Introduction

There is considerable interest in the development of treatment protocols for chronic myeloid leukemia (CML) that includes the possibility of tyrosine kinase inhibitor (TKI) therapy cessation in patients who achieve durable deep molecular response (DMR) i.e., MR4 or better [1]. Treatment-free remission (TFR) has been assessed in controlled clinical studies [2-8]. A critical part of these trials is frequent molecular monitoring based on the quantification of *BCR-ABL1* transcripts, expressed on the international scale (IS) [9]. In most TKI cessation trials, patients are eligible to stop treatment if they have been in DMR for at least 2 years. Patients are frequently monitored after treatment cessation during the first year, and in cases of a loss of major molecular response (MMR; >0.1% *BCR-ABL1* IS), TKI treatment is restarted. Data from TKI cessation trials have shown that 40-60% of patients maintain DMR after TKI discontinuation [2-8, 10-12]. Molecular relapses occur within the first 6 months after TKI cessation in the majority of patients who failed to maintain DMR.

BCR-ABL1-positive leukaemia stem cells (LSCs) may persist in some patients with long-term *BCR-ABL1* mRNA negativity on imatinib treatment [13]. This is not explained by the lack of BCR-ABL1 kinase inhibition but is related to quiescence, enhanced survival and microenvironmental protection. Current research focuses on identifying parameters that indicate which CML patients have a high probability of sustaining TFR. The quantity of residual LSCs may be more precisely measured by genomic DNA analysis, potentially providing clearer eligibility for TKI cessation [14]. It is evident that the duration of DMR and of TKI therapy before cessation are associated with TFR [2, 11]. Additionally, patients who failed to achieve early molecular response (EMR) had the poorest achievement of stable DMR after 8 years of imatinib therapy [15]. A better understanding of disease dynamics in terms of mathematical and quantitative models can further help to identify patients for whom TKI cessation represents a promising treatment alternative [16].

In some cases, *BCR-ABL1* DNA quantification may indicate the persistence of leukemic cells despite the undetectable *BCR-ABL1* expression [17]. DNA based monitoring may enable the discovery of “hidden” CML cells such as quiescent LSCs or lymphoid cells [18], and low *BCR-ABL1* expression

may potentially enable the persistence of LSCs under TKI treatment [19, 20]. In this collaborative European Treatment and Outcome Study for CML (EUTOS) work, the patient-specific quantitative DNA MRD assays were established to determine whether DNA-based monitoring may have clinical relevance in CML, especially in relation to TFR.

Materials and Methods

The detailed version is provided as Supplementary Materials and Methods.

Patient cohorts

The first cohort consisted of 81 newly diagnosed CML patients enrolled within the years 2016-2018 (Table S1) who had given their consent for frequent visits during the first 6 months of TKI therapy according to the time schedule shown in Figure S1A. The *BCR-ABL1* genomic fusions were successfully characterized in all patients from the first cohort (n=81).

The second cohort consisted of 87 patients who achieved and maintained DMR during long-term treatment. The breakpoints could not be characterized in 10/87 cases (primarily due to unavailability of suitable DNA), leaving 77 for analysis. The clinical and biological characteristics (age, response to TKI, duration of TKI treatment) of the 10 patients did not differ from the 77 included cases (Table S2). Of these 77 patients, 35 continued with TKI therapy, while 17 were included in the EURO-SKI study (Europe Stops TKI in CML) and ceased treatment. The remaining 25 patients, who fulfilled the cessation criteria but could not be involved in the EURO-SKI trial, gave consent for an intermittent regimen (INTReg) of TKI administration every second month. The molecular relapse-free survival (MRFS) rate of INTReg patients was comparable to that reported in the EURO-SKI at later time points (48% at 24 months; Figure S2) [2]. In the case of MMR loss (n=13), a full daily dose of TKI was reintroduced. All 13 patients re-achieved DMR. In one of these cases, TKI therapy was completely withdrawn after 30 months of TKI reintroduction, and the patient remains in DMR 36 months later. One patient died from myocardial infarction in DMR. The remaining 12 patients with

sustained DMR remained on TKI every second month for a median 20 months since INTReg start (range 13-86 months). The therapy was completely stopped in one patient after 58 months in DMR, with DMR sustained for 12 months to date. Two of the 12 patients died from colon cancer and myocardial infarction, respectively.

Patient-specific genomic *BCR-ABL1* fusion characterization

Patient-specific DNA *BCR-ABL1* fusions were characterized in 158 (81+77) patients from both cohorts using two approaches. The first approach was based on long-distance PCR (LD-PCR) and was described previously [21]. The second approach was based on next-generation sequencing (NGS) using the Illumina platform and the Rapid Capture Custom Enrichment approach (Illumina, San Diego, CA, USA), which includes 4608 probes covering genomic regions of the *BCR* gene and the *ABL1* gene, including upstream and downstream regions. The manufacturers' protocols were followed for sample and library preparation. MiSeq Reagent Kit v3 was used for sequencing performance (Illumina). The observed reads in fastq format were evaluated using NextGENe (Softgenetics, State College, PA, USA).

Real-time qPCR (qPCR)

DNA and RNA were extracted from the same amount of white blood cells (5-20x10^6) isolated from the peripheral blood and bone marrow samples.

DNA qPCR

Primers and probes were designed and passed PCR quality criteria for 148 of 158 patient-specific *BCR-ABL1* fusions. The ten patients for whom adequate qPCR could not be designed were all from the first cohort of prospectively analysed CML patients.

The rules for patient-specific DNA qPCR analysis were adopted from the recommendation of the EURO-MRD consortia for patient-specific Ig/TCR rearrangement analysis. The albumin (*ALB*) gene

was applied as a control gene with standardized primers and probes [22]. As negative controls, DNAs from 6 healthy donors were analysed as single reactions or DNAs from 3 healthy donors as duplicates. Patient samples with *BCR-ABL1* transcripts > 0.01% IS (known from the routine *BCR-ABL1* mRNA transcript monitoring) were measured in duplicate, and patient samples with *BCR-ABL1* transcripts < 0.01% IS were measured in triplicate.

mRNA qPCR

BCR-ABL1 qPCR at the transcript level was performed using *GUSB* as a control gene and with primers and probes that are used for standardized monitoring [9]. Certified ERM-AD623 (Sigma-Aldrich, St Louis, MO, USA) standards were used to determine the copy numbers of *BCR-ABL1* and *GUSB*. In each qPCR run, 2 negative (healthy donor and no template control) and 2 positive controls (samples with 1% and 0.01% *BCR-ABL1* IS prepared from K562 cell line) were analysed. Patient samples with *BCR-ABL1* transcripts > 0.01% IS were measured in duplicate, and patient samples with *BCR-ABL1* transcripts < 0.01% IS were measured in triplicate. The *BCR-ABL1* level on the IS was determined from the standardized monitoring of *BCR-ABL1* that preceded the mRNA and DNA measurements applied in this study.

Droplet digital PCR (ddPCR)

ddPCR was performed using the QX200 AutoDG Droplet Digital PCR System (Bio-Rad, Hercules, CA, USA). The maximum concentration of DNA allowed to perform ddPCR was 100 ng/µl. The reaction mixture preparation and conditions were applied according to the recommendations of the manufacturer (Bio-Rad). Patient samples were analysed in quadruplicate. Six negative controls (healthy donors) were applied for each patient-specific assay. Samples with <10 000 droplets were discarded from the analysis.

ddPCR of *BCR-ABL1* transcripts was performed using the primers and probes used for qPCR. The copy number of *GUSB* was analysed by qPCR due to the high expression of *GUSB*, which exceeds

180 the limit allowed for ddPCR analysis. Samples were analysed in quadruplicate. Each ddPCR run included
181 2 positive controls and 1 negative control. The reaction mixture preparation and conditions were
182 applied according to the manufacturer's recommendations (Bio-Rad).
183
184 **DNA and mRNA *BCR-ABL1* data evaluations**
185 The quantity of *gBCR-ABL1* (genomic *BCR-ABL1*) from qPCR analysis was determined in
186 relation to the corresponding quantity in the diagnostic sample (the level of *gBCR-ABL1* in this
187 sample was defined as 100%) using the following calculations:
188 1) % *gBCR-ABL1*= (⌀ concentration *BCR-ABL1* DNA)/(⌀ concentration of total DNA (*ALB*))*100
189 2) % $gBCR\text{-}ABL1_{RelDg}$= (% $gBCR\text{-}ABL1_{sample}$)/(% $gBCR\text{-}ABL1_{Dg}$)*100.
190 For the reliable comparison of qPCR and ddPCR approaches, the quotations used for ddPCR data
191 evaluations were as follows:
192 1) % *gBCR-ABL1* sample= (⌀ copy number of *gBCR-ABL1*)/(⌀ copy number of *ALB*)*100
193 2) % $gBCR\text{-}ABL1_{RelDg}$= (% $gBCR\text{-}ABL1_{sample}$)/(% $gBCR\text{-}ABL1_{Dg}$)*100.
194
195 For the reliable comparison of mRNA and DNA *BCR-ABL1* data, mRNA *BCR-ABL1* data were also
196 related to the level of the diagnostic sample, which was defined as 100%. Stringent quality
197 requirements were established to exclude poor-quality samples from the evaluations (Table 1).
198
199 **Statistical analysis**
200 For bi-exponential mixed effect models, all *BCR-ABL1* levels were log-transformed. Negative and
201 positive *BCR-ABL1* levels outside the quantifiable range (POQR) were treated as left-censored
202 observations with global or individual upper quantification limits (QL) at DNA or mRNA level,
203 respectively. The type of TKI (imatinib vs nilotinib), TKI dose (full dose vs low dose) and the transcript
204 type (e13a2 vs e14a2) were further included as additional covariates in the models, in which they
205 were represented as fixed effects of the α and β slopes, assuming the same model structure as

published in Glauche et al. [23]. Wald tests were applied to assess the statistical significance of the fixed effect group effects. The software "Monolix" (version 2018R2) (lixoft.com/products/monolix/) was used. The correlation of the estimated parameters between DNA- and mRNA-based measurements was quantified using Pearson's correlation coefficient.

The cumulative incidences of molecular relapse free survival (MRFS) after TKI stop/interruption were depicted using the Kaplan-Meier method. All the curves are presented with 95% confidence intervals (CIs). Differences in cumulative incidences between patient groups were assessed using the log-rank test. The follow-up was defined from the date of TKI cessation to the date of molecular relapse or the end of follow-up, whichever came first. An event was defined as the occurrence of molecular relapse. The Cox regression was used to estimate the effect of transcript type, of duration of TKI and DMR on MRFS. All tests were two-sided, as the analyses were considered exploratory, and no correction for multiple testing was performed. To statistically demonstrate the superiority of DNA and/or RNA *BCR-ABL1* for TFR prediction, the Cox model was fitted using a forward stepwise variable selection process. The deterministic model to identify patterns of DNA and RNA results during DMR before TKI stop/interruption was developed using INTReg data and validated using EURO-SKI data. For all analyses, p-values<0.05 were considered statistically significant.

Results

BCR-ABL1 genomic fusion characterization

BCR-ABL1 patient-specific fusions of 158 patients were identified (Table S3) using different methods. While *BCR-ABL1* genomic fusions were successfully characterized in 124 patients using LD-PCR [19], this method failed for 24 patients, which could only be characterized by the NGS approach. Additional 10 *BCR-ABL1* fusions were directly characterized by NGS without attempting LD-PCR. In 7/34 patients characterized by NGS, the breaks were localized upstream from *ABL1* and downstream from *EXOSC2*. In one case, the genomic fusion *BCR-ASIC2-ABL1* was discovered, which corresponded to the cytogenetic observation [46, XX, t(9;22;17) (q34;q11;q21)]. A 4.8-kbp sequence of intron 1 of

ASIC2 (chromosome 17) was inserted between *BCR* intron 14 and *ABL1* intron 1. The splicing of the *BCR-ASIC2-ABL1* fusion gene leads to e14a2 *BCR-ABL1* formation.

In 3 patients, both transcript types (e13a2 and e14a2) were detected at the time of diagnosis. In all 3 patients, only one *BCR-ABL1* genomic fusion was found resulting from breaks in *BCR* intron 14 and *ABL1* intron 1b.

The amount of mRNA and DNA *BCR-ABL1*$_{\text{RelDG}}$ at the sample level highly correlated from the start of TKI until achievement of DMR

The quantity of *BCR-ABL1*$_{\text{RelDG}}$ was compared at the DNA and mRNA levels in each patient's sample that was available for DNA- and mRNA-based analyses. DNA and mRNA levels were analysed by qPCR in 2189 peripheral blood samples (129 patients) and by ddPCR in 1279 peripheral blood samples (62 patients). Results for all assays that passed the quality criteria were considered as positive for *BCR-ABL1*, quantifiable; positive for *BCR-ABL1* outside the quantifiable range (POQR) or negative for *BCR-ABL1* (Table 1). Stringent quality requirements (Table 1) ensured a reliable comparison of mRNA and DNA data at the same level of technical sensitivity, corresponding to MR4-MR5 and 10^{-4}–10^{-5}, respectively.

The mRNA and DNA levels (both related to the diagnostic level) of *BCR-ABL1*$_{RelDg}$ were highly correlated in samples with quantifiable *BCR-ABL1* by both methods (qPCR r=0.93, Figure 1A; ddPCR r=0.89, Figure 1B). Discordant results (undetectable RNA/POQR DNA; undetectable RNA/quantifiable DNA; POQR RNA/undetectable DNA; POQR RNA/quantifiable DNA; quantifiable RNA/undetectable DNA; quantifiable RNA/POQR DNA) were found in 674/2189 samples measured by qPCR and in 585/1279 samples measured by ddPCR. DNA-qPCR provided quantifiable or POQR *BCR-ABL1* compared to POQR or negative *BCR-ABL1* by mRNA-qPCR in 91% of discordant samples. *BCR-ABL1* was quantifiable by DNA-ddPCR in 97% of discordant samples that were *BCR-ABL1* POQR or negative by mRNA-ddPCR.

In 64/128 patients the number of *BCR-ABL1* positive samples by qPCR-DNA was higher compared to qPCR-mRNA (Figure S3A). By ddPCR the higher number of *BCR-ABL1* positive samples on DNA level compared to mRNA was found in 56/61 patients (Figure S3B).

A total of 1032 samples (43 patients) were available for comparison of mRNA analysis by qPCR and ddPCR (Figure S4). Of these, 846 results were considered concordant (undetectable BCR-ABL1 on DNA and RNA level; POQR DNA and RNA; quantifiable DNA and RNA). Of the 186 discordant samples, 93% of samples that were quantifiable or POQR by ddPCR were either POQR or negative by qPCR. DNA *BCR-ABL1* levels were concordant by both techniques in 62% of 864 analysed samples. Of the 325 discordant samples, 87% were *BCR-ABL1* quantifiable by ddPCR-DNA, while POQR or negative by qPCR.

To further understand the sensitivity of mRNA versus DNA analysis, $BCR\text{-}ABL1_{RelDg}$ qPCR data were compared in samples with comparable levels of sensitivity (n=1383) according to the control gene copy number and corresponding to MR4-MR4.5 (mRNA) and 10^{-4} (DNA), respectively. Of these, 1066 results were considered concordant (Figure S5). Discordant results were found in 317/1383 samples. DNA-qPCR provided quantifiable or POQR *BCR-ABL1* compared to POQR or negative *BCR-ABL1* by mRNA-qPCR in 89% of discordant samples.

Individual dynamics of $BCR\text{-}ABL1_{RelDg}$ at the DNA and mRNA levels highly correlated during initial decline after TKI start

TKI therapy induces a biphasic decline in *BCR-ABL1* transcript levels, characterized by an initially steep decline (α slope) followed by a moderate decline (β slope) in CML patients responding to first-line TKI treatment. The separate bi-exponential mixed effects models were applied for DNA and mRNA *BCR-ABL1* to study differences between DNA and mRNA $BCR\text{-}ABL1_{RelDg}$ dynamics during first-line TKI therapy considering the effects of the TKI dose, type of TKI and transcript type in the cohort of newly diagnosed CML patients (Table S1). DNA patient-specific assays were successfully applied in 71/81 patients. Four patients were excluded due to a quick TKI change after the start of first-line TKI

283 treatment (1 patient), a combination therapy with interferon alpha (2 patients) or higher than normal
284 TKI doses (1 patient). The median follow-up time from TKI start for first-line therapy in 67 newly
285 diagnosed patients was 20.7 months (range 0.5-35.2 months). Forty-two patients (62.7%) achieved
286 MMR within a median of 9.1 months after the start of TKI treatment (range 2.5-34.9). The bi-
287 exponential mixed effects models showed a high correlation of the individual parameter estimates
288 between mRNA- and DNA-based measurements, especially for the α slope and the intercept B,
289 indicating that the overall dynamics are described equally well by both methods (Figure 2). A lower
290 correlation for the β slope may be explained by observed differences in the sensitivity of MRD
291 measurements between mRNA- and DNA-based analysis.
292 The TKI type significantly impacts on the individual α slopes (Figure 3A) at both the mRNA and the
293 DNA level while TKI dose influences the β slope (Figure 3B) at DNA level only. No differences were
294 found in the individual dynamics of mRNA and DNA for the transcript type (Figure 3C). Especially with
295 respect to the dose effect on the β slope the caution is warranted as after the removal of patients
296 with atypical responses (such a slow initial remission, recurrence and too few data points) this effect
297 cannot be confirmed with the required level of significance.
298
299 **DNA-based *BCR-ABL1* analysis during DMR maintenance impacts the probability of TFR**
300 We aimed to assess whether DNA-based *BCR-ABL1* analysis may be a better predictor of TFR
301 compared to mRNA analysis. DNA and mRNA *BCR-ABL1* levels from consecutive analyses before and
302 after TKI cessation/interruption were available for 42 patients (total 1108 samples; median 24
303 samples per patient; range 11-44) in whom TKI treatment was ceased (EURO-SKI; n=17) or
304 interrupted (INTreg; n=25) (Table S2). A mathematical model was established to identify patterns of
305 DNA and RNA results during DMR. For each patient, the model evaluated *BCR-ABL1* positivity or
306 negativity on the DNA and RNA levels and considered the level of sensitivity for each sample. The
307 scheme of the model is provided on Figure S6. Using the model, 3 groups of patients were identified:
308 1) a group with double *BCR-ABL1* negative pattern (EURO-SKI n=5, median time 55 months before TKI

cessation, range 13-105 months; INTReg n=6, median time 32 months before INTReg, range 15-49 months); 2) a group with DNApos/RNAneg *BCR-ABL1* pattern (EURO-SKI n=7, median time 35 months before TKI cessation, range 8-88 months; INTReg n=9, median time 35 months before INTReg, range 8-82 months); and 3) a group of patients with double positive *BCR-ABL1* pattern (EURO-SKI n=5, median time 29 months before TKI cessation, range 16-34 months; INTReg n=10, median time 29 months before INTReg, range 9-68 months). There was no case with DNAneg/RNApos *BCR-ABL1* pattern. The MRFS rate was evaluated in each group after TKI cessation/interruption (Figure 4). The MRFS rate for group 1 was 80% (median follow-up 61 months; range 41-70) and 100% (median follow-up 60 months; range 13-77), respectively. Four EURO-SKI and 6 INTReg patients from group 1 sustained MRFS with a continuous double negative status. Two of these patients gave consent for bone marrow (BM) aspiration at the time of TKI cessation. All harvested cells were split into two equal aliquots for DNA and RNA isolation, respectively, and entire samples were analysed in these patients, corresponding to an analysis of 0.43 and 6.5 million BM cells, by both DNA and mRNA ddPCR. Both BM samples were double negative by ddPCR analysis.

The lowest rate (20%) of MRFS occurred for group 3. In group 2, 8 cases (4/7 EURO-SKI patients and 4/9 INTreg patients) continued without molecular relapse after TKI cessation/interruption (median 62 months, range 53-71 months and median 47 months, range 19-71 months, respectively); in 3 of the 8 patients (2 EURO-SKI, 1 INTReg) *BCR-ABL1* expression became detectable but only at DMR levels (i.e., MR4-MR5). *BCR-ABL1* expression remained undetectable in 5 of the 8 patients (2 EURO-SKI, 3 INTReg) after TKI cessation. BM was collected in 2 of these patients at the time of TKI cessation. Again, all harvested cells were split into two equal aliquots for DNA and RNA isolation, respectively, and entire samples were analysed by ddPCR, corresponding to an analysis of 6.2 million and 10 million BM cells. In both cases DNA assays detected residual CML cells despite the absence of *BCR-ABL1* expression, which corresponded to the observation in the peripheral blood.

Based on the identification of 3 distinct groups of patients who differed according to the MRFS rate (Figure 4) we propose a “traffic light” model of patient stratification according to DMR

status before TKI cessation: the double negative group is “green”, the DNApos/RNAneg group is “yellow”, and the double positive group is “red”. Because of the similarity of both cohorts, we performed analysis of the probability of MRFS according to the traffic light stratification on a cohort including EURO-SKI and INTReg patients (Figure 5). The probability of MRFS according to the traffic light stratification showed significant differences ($p< 0.001$) between the groups, with 100% MRFS at 18 months since TKI cessation/interruption in the green group, 63% (OR 0.388-0.862) in the yellow and 20% in the red group (OR 0-0.402). The two cohorts showed the same pattern of MRFS when analysed separately (Figure S7). The probability of MRFS according to the traffic light stratification showed significant differences in the cohort of INTReg patients ($p=0.005$) with 100% MRFS at 18 months since TKI interruption in the green group, 67% (OR 0.359-0.974) in the yellow and 20% in the red group (OR 0-0.447) (Figure S7A). Although not significant, similar marked differences were found in the EURO-SKI group of patients in the probability of MRFS according to the traffic light model with 80% MRFS at 18 months since TKI cessation in the green group, 57% (OR 0.217-0.930) in the yellow and 20% (OR 0-0.551) in the red group (Figure S7B). The ratio between the duration of DMR and duration of treatment before cessation/interruption was related to the probability of remaining in TFR (INTReg $p= 0.006$, HR 1.473 (CI 95% 1.120; 1.936); EURO-SKI $p=0.175$, HR 2.429 (CI 95% 0.683; 8.638), not significant due to the low power). There was no significant impact of the transcript type (e13a2=14; e14a2=28).

Additionally, a forward conditional Cox model was applied to demonstrate what parameter (*BCR-ABL1* DNA and/or RNA patterns during DMR maintenance before TKI stop evaluated by the deterministic model; Figure S6) has superiority for TFR prediction. The analysis was performed on EURO-SKI and INTReg patients. The sole parameters RNA or DNA showed similar likelihood for prediction of TFR (Table S4). The use of both parameters together significantly increased the prediction power ($p<0.001$) and the model fit was also better (as indicated by a significant decrease in -2Log likelihood). Thus, the model with both RNA and DNA parameters was superior to the model with RNA or DNA as solo parameters.

Finally, the value of the model was assessed by calculating the sensitivity, specificity, positive predictive value (PPV) and negative predictive value (NPV) for (a) the green group versus yellow+red, and (b) for green+yellow versus red (Table S5). The highest specificity (0.95) and PPV (0.91) was seen for (a), whereas the highest sensitivity (0.86) and NPV (0.8) was seen for (b).

Discussion

At present, an important initiative in CML is a definition of a treatment-free remission score (TFR-score). Several parameters seem to be promising, including the duration of TKI and the maintenance of DMR before TKI cessation. Other characteristics, including specific immune profiles, and the DNA-based detection of residual CML cells, are currently under investigation [24-26].

In this EUTOS work, the aim was to determine at which phases of disease course during TKI therapy the DNA-based monitoring of *BCR-ABL1* may be important, especially in relation to TFR. The NGS-based approach has been established for the identification of a patient-specific *BCR-ABL1* genomic fusion. The large set of designed probes (n=4608) was applied to enhance the probability of detecting the majority of genomic *BCR-ABL1* fusions. DNA-based approaches were carefully set up for qPCR and ddPCR analyses. The initial number of cells used was the same for DNA and mRNA isolation in each sample analysed to be able to reliably compare both types of analyses. The conditions and criteria for qPCR and the rules for MRD evaluations of mRNA and DNA *BCR-ABL1* measurements were adopted according well standardized method for quantification of the patient-specific Ig/TCR rearrangement by the international consortia EURO-MRD [22].

This work showed that DNA *BCR-ABL1* levels highly correlated with mRNA levels in CML samples at levels ≥ 0.01% *BCR-ABL1*$_{\mathrm{RelDg}}$, which is in concordance with Pagani et al. [26]. The investigated comparison of DNA and mRNA *BCR-ABL1* quantity at the patient level using the bi-exponential mixed effects models showed no difference between DNA and mRNA individual dynamics in *BCR-ABL1* during the initial decline after TKI start. As expected, the steepness of the first decline in either DNA or mRNA *BCR-ABL1* was significantly influenced by the type of TKI, but the

effect of transcript type (e13a2 vs e14a2) or TKI dose was not found. Nilotinib depleted the number of CML proliferating cells faster than did imatinib. However, a similar correlation of the TKI type with the dynamics of long-term decline could not be identified [23]. As discussed previously, this observation may result from the fact that TKI toxicity determines the initial treatment response, while the long-term dynamics are governed by the slow activation of less sensitive LSCs with low turnover [27-29]. This may explain why even though the rate of MMR achievement is significantly higher and faster in patients treated with second-generation TKIs compared to imatinib, the overall outcome with respect to progression or survival does not differ [30].

Discrepancies between mRNA and DNA *BCR-ABL1* levels were frequently found at *BCR-ABL1*$_{\text{RelDg}}$ below 0.01%. DNA based *BCR-ABL1* analyses detected residual CML cells compared to mRNA analysis in a significant number of samples in patients during their follow-up. With the methodology used the technical sensitivity of the DNA and RNA approaches were indistinguishable. Thus, the higher "sensitivity" of DNA *BCR-ABL1* analysis corresponds to biological rather than technical reasons. In particular, an interesting group of patients was that in whom *BCR-ABL1* was detected in the majority of samples collected at the time of DMR maintenance using patient-specific genomic *BCR-ABL1* assays but at the transcript level, *BCR-ABL1* was negative. This observation may be important when addressing the probability of TFR. The cohort of 42 patients in whom TKI therapy was ceased (EURO-SKI) interrupted (INTReg) was investigated. MRD was analysed with mRNA- and DNA-ddPCR during DMR maintenance before and after TKI cessation/interruption. The combined DNA and mRNA *BCR-ABL1* pattern (evaluated by the deterministic model) during DMR maintenance allowed a "traffic light" stratification that significantly associated with MRFS after TKI cessation or interruption. The yellow group is interesting from a biological; point of view, especially in patients with detectable *BCR-ABL1*-positive cells, which do not express *BCR-ABL1* after TKI cessation. It would be interesting to characterize this type of cell in further studies. Recently, Pagani et al. showed that in patients in TFR with undetectable *BCR-ABL1* transcript, *BCR-ABL1* DNA positivity was confined to

412 the lymphoid compartment [18]. The authors suggested that MRD in the blood of TFR patients need
413 not imply the persistence of multipotent CML cells.
414 The variables associated with MRFS in the studied group was the duration of DMR before TKI
415 cessation/interruption and the proportion between the duration of DMR and treatment.
416 This work showed that the DNA-based measurement of *BCR-ABL1* does not provide any novel
417 information compared with the mRNA-based measurement during the initial rapid decline in *BCR-*
418 *ABL1* after the start of TKI treatment. However, during DMR maintenance, DNA-based analysis may
419 be very helpful, especially in the prediction of TFR. This study proposes a "traffic light" stratification
420 as a promising TFR predictor to estimate the likelihood of successfully achieving sustained TFR: green
421 indicates a high probability of achieving TFR, yellow indicates an intermediate probability of
422 achieving TFR, and red indicates a low probability of achieving TFR. A further work should aim to
423 evaluate the utility of this traffic light model in conjunction with other parameters (e.g.,
424 immunological profiles, duration of DMR and TKI therapy) as well as the potential for improving TFR
425 rates by the use of dose reduction in the yellow and red groups.
426

427 **Acknowledgement**

428 This work was funded by the Project Grant #15-31540A and #16-30186A from the Czech Health
429 Research Council and by the European Treatment and Outcome study (EUTOS) for CML. The authors
430 thank for the institutional support #00023736 (Institute of Hematology and Blood Transfusion) and
431 #00064203 (University Hospital Motol) from Ministry of Health of the Czech Republic and the Czech
432 Leukemia Study Group for Life. This work was further supported by ERA-Net ERACoSysMed JTC-2
433 project "prediCt" (project number 031L0136A) to IR. We would like to thank to Dr. Milada Småstuen
434 (Oslo Metropolitan University) for the consolations on statistical analysis. The authors are grateful to
435 the patients for providing their samples for this study.
436

437 **Author contributions**

KMP designed the study, interpreted results and wrote the paper; HZ and EM performed ddPCR and qPCR analyses, analysed data and provided data management; JZ supervised DNA PCR analysis, contributed to the writing of the paper; LH performed LD-PCR and characterised DNA *BCR-ABL1* fusions; AG and IG performed statistical analysis using bi-exponential mixed effect models, interpreted results and reviewed the paper; JK performed bioinformatics of NGS data, designed primers and probes; PP performed statistical analysis; HK, MSM and DS supervised patient's visits, evaluated and provided clinical data; AB and VP performed NGS analysis; TJ performed qPCR analysis; DZ and JM supervised patient's visits, evaluated and provided clinical data; TE designed probes for NGS analysis; FXM and SS supervised the EURO-SKI study; IR supervised statistical analysis, advised the concept of the paper and critically reviewed the paper; NCPC contributed to the concept of the paper and the paper writing; AH supervised the work; All authors critically reviewed and approved the paper.

Competing Interests

KMP, TE, NCPC, AH received support by Novartis through the European Treatment and Outcome Study (EUTOS) for CML.

Ethical Statement

This work was conducted in accordance with the principles of the Declaration of Helsinki and was approved by the Ethics Committees of the Institute of Hematology and Blood Transfusion, Prague and Faculty Hospital Brno. All patients provided written informed consent for the use of their samples for this research.

References

1. Cross NC, White HE, Colomer D, Ehrencrona H, Foroni L, Gottardi E, Lange T, et al. Laboratory recommendations for scoring deep molecular responses following treatment for chronic myeloid leukemia. Leukemia. 2015;29:999-1003.

2. Saussele S, Richter J, Guilhot J, Gruber FX, Hjorth-Hansen H, Almeida A, et al. Discontinuation of tyrosine kinase inhibitor therapy in chronic myeloid leukaemia (EURO-SKI): a prespecified interim analysis of a prospective, multicentre, non-randomised, trial. Lancet Oncol. 2018;19:747-757.

3. Shah N, Gutiérrez JVG, Jiménez-Velasco A, Larson SE, Saussele S, Rea D, et al. Updated 18-Month Results from Dasfree: A study evaluating dasatinib discontinuation in patients with dhronic myeloid leukemia in chronic phase and deep molecular response. Blood. 2018;132:4253.

4. Clark RE, Polydoros F, Apperley JF, Milojkovic D, Pocock C, Smith G, et al. De-escalation of tyrosine kinase inhibitor dose in patients with chronic myeloid leukaemia with stable major molecular response (DESTINY): an interim analysis of a non-randomised, phase 2 trial. Lancet Haematol. 2017;4:e310–e316.

5. Mori S, Vagge E, le Coutre P, Abruzzese E, Martino B, Pungolino E, et al. Age and dPCR can predict relapse in CML patients who discontinued imatinib: the ISAV study. Am J Hematol. 2015;90:910–914.

6. Ross DM, Masszi T, Gómez Casares MT, Hellmann A, Stentoft J, Conneally E, et al. Durable treatment-free remission in patients with chronic myeloid leukemia in chronic phase following frontline nilotinib: 96-week update of the ENESTfreedom study. J Cancer Res Clin Oncol. 2018;144:945-954.

7. Mahon FX, Boquimpani C, Kim DW, Benyamini N, Clementino NCD, Shuvaev V, et al. Treatment-free remission after second-line nilotinib treatment in patients with chronic myeloid leukemia in chronic phase: results from a single-group, phase 2, open-label study. Ann Intern Med. 2018;168:461-470.

8. Nicolini FE, Dulucq S, Boureau L, Cony-Makhoul P, Charbonnier A, Escoffre-Barbe M, et al. The Evaluation of Residual Disease By Digital PCR, and TKI Duration Are Critical Predictive Factors for Molecular Recurrence after for Stopping Imatinib First-Line in Chronic Phase CML Patients: Results of the STIM2 Study. Blood. 2018;132:462.

9. Cross NC, White HE, Müller MC, Saglio G, Hochhaus A. Standardized definitions of molecular response in chronic myeloid leukemia. Leukemia. 2012;26(10): 2172-5.

10. Mahon FX, Réa D, Guilhot J, Guilhot F, Huguet F, Nicolini F, et al. Discontinuation of imatinib in patients with chronic myeloid leukaemia who have maintained complete molecular remission for at least 2 years: the prospective, multicentre Stop Imatinib (STIM) trial. Lancet Oncol. 2010;11:1029-1035.

11. Ross DM, Branford S, Seymour JF, Schwarer AP, Arthur C, Yeung DT, et al. Safety and efficacy of imatinib cessation for CML patients with stable undetectable minimal residual disease: results from the TWISTER study. Blood. 2013;122:515–522.

12. Imagawa J, Tanaka H, Okada M, Nakamae H, Hino M, Murai K, et al. Discontinuation of dasatinib in patients with chronic myeloid leukaemia who have maintained deep molecular response for longer than 1 year (DADI trial): a multicentre phase 2 trial. Lancet Haematol. 2015;2:e528–e535.

13. Chu S, McDonald T, Lin A, Chakraborty S, Huang Q, Snyder DS, et al. Persistence of leukemia stem cells in chronic myelogenous leukemia patients in prolonged remission with imatinib treatment. Blood. 2011;118:5565-5572.

14. Ross DM, Branford S, Seymour JF, Schwarer AP, Arthur C, Bartley PA, et al. Patients with chronic myeloid leukemia who maintain a complete molecular response after stopping imatinib treatment have evidence of persistent leukemia by DNA PCR. Leukemia. 2010;24:1719–1724.

15. Branford S, Yeung DT, Ross DM, Prime JA, Field CR, Altamura HK, et al. Early molecular response and female sex strongly predict stable undetectable *BCR-ABL1*, the criteria for imatinib discontinuation in patients with CML. Blood. 2013;121:3818-3824.

16. Horn M, Glauche I, Müller MC, Hehlmann R, Hochhaus A, Loeffler M, et al. Model-based decision rules reduce the risk of molecular relapse after cessation of tyrosine kinase inhibitor therapy in chronic myeloid leukemia. Blood. 2013;121:378-384.

17. Ross DM, Pagani IS, Shanmuganathan N, Kok CH, Seymour JF, Mills AK, et al. Long-term treatment-free remission of chronic myeloid leukemia with falling levels of residual leukemic cells. Leukemia. 2018;32:2572-2579.

18. Pagani IS, Dang P, Saunders VA, Grose R, Shanmuganathan N, Kok CH, et al. Lineage of measurable residual disease in patients with chronic myeloid leukemia in treatment-free remission. Leukemia 2019 Nov 25. doi: 10.1038/s41375-019-0647-x. [Epub ahead of print]

19. Kumari A, Brendel C, Hochhaus A, Neubauer A, Burchert A. Low BCR-ABL expression levels in hematopoietic precursor cells enable persistence of chronic myeloid leukemia under imatinib. Blood. 2012;119:530–539.

20. Chomel JC, Sorel N, Guilhot J, Guilhot F, Turhan AG. BCR-ABL expression in leukemic progenitors and primitive stem cells of patients with chronic myeloid leukemia. Blood. 2012;119:2964–2965.

21. Hovorkova L, Zaliova M, Venn NC, Bleckmann K, Trkova M, Potuckova E, et al. Monitoring of childhood ALL using *BCR-ABL1* genomic breakpoints identifies a subgroup with CML-like biology. Blood. 2017;129:2771-2781.

22. van der Velden VH, Cazzaniga G, Schrauder A, Hancock J, Bader P, Panzer-Grumayer ER, et al. Analysis of minimal residual disease by Ig/TCR gene rearrangements: guidelines for interpretation of real-time quantitative PCR data. Leukemia. 2007;21:604-611.

23. Glauche I, Kuhn M, Baldow C, Schulze P, Rothe T, Liebscher H, et al. Quantitative prediction of long-term molecular response in TKI-treated CML - Lessons from an imatinib versus dasatinib comparison. Sci Rep. 2018. 8:12330.

539 24. Ilander M, Olsson-Strömberg U, Schlums H, Guilhot J, Brück O, Lähteenmäki H, et al. Increased
540 proportion of mature NK cells is associated with successful imatinib discontinuation in chronic
541 myeloid leukemia. Leukemia. 2017;31:1108–1116.
542 25. Schütz C, Inselmann S, Sausslele S, Dietz CT, Müller MC, Eigendorff E, et al. Expression of the
543 CTLA-4 ligand CD86 on plasmacytoid dendritic cells (pDC) predicts risk of disease recurrence after
544 treatment discontinuation in CML. Leukemia. 2017;32:1–8.
545 26. Pagani IS, Dang P, Kommers IO, Goyne JM, Nicola M, Saunders VA, et al. *BCR-ABL1* genomic DNA
546 PCR response kinetics during first-line imatinib treatment of chronic myeloid leukemia.
547 Haematologica. 2018;103:2026-2032.
548 27. Fassoni AC, Baldow C, Roeder I, Glauche I. Reduced tyrosine kinase inhibitor dose is predicted to
549 be as effective as standard dose in chronic myeloid leukemia: a simulation study based on phase III
550 trial data. Haematologica. 2018;103:1825-1834.
551 28. Roeder I, Horn M, Glauche I, Hochhaus A, Mueller MC, Loeffler M. Dynamic modeling of imatinib-
552 treated chronic myeloid leukemia: functional insights and clinical implications. Nat Med.
553 2006;12:1181-1184.
554 29. Wilson A, Laurenti E, Oser G, van der Wath RC, Blanco-Bose W, Jaworski M, et al. Hematopoietic
555 stem cells reversibly switch from dormancy to self-renewal during homeostasis and repair. Cell.
556 2008;135:1118-1129.
557 30. Hochhaus A, Saglio G, Hughes TP, Larson RA, Kim DW, Issaragrisil S, et al. Long-term benefits and
558 risks of frontline nilotinib vs imatinib for chronic myeloid leukemia in chronic phase: 5-year update of
559 the randomized ENESTnd trial. Leukemia. 2016. 30:1044–1054.
560

561 **Legend to the figures:**

562 **Figure 1. Comparison of *BCR-ABL1*$_{\text{RelDg}}$ data at mRNA and DNA levels.** (A) Comparison of *BCR-*
563 *ABL1*$_{\text{RelDg}}$ mRNA and DNA levels in CML patients using qPCR (2189 samples from 129 patients). The
564 red line represents 100% concordance and dashed red lines delineate the area of 95% confidence. In

565 total, 1051/2189 samples were quantifiable by qPCR on both DNA and mRNA, with majority of
566 samples (96%) at levels ≥ 0.01% of *BCR-ABL1*$_{RelDg}$. qPCR-DNA and -mRNA analyses were both *BCR-*
567 *ABL1* POQR in 40 samples and both negative in 424 samples. From remaining 674/2189 samples
568 measured by qPCR, 360 samples (53%) were *BCR-ABL1* DNA quantifiable and POQR or negative by
569 mRNA, and 252 samples (37%) were DNA POQR and negative by mRNA. Only 37/674 samples (6%)
570 were *BCR-ABL1* quantifiable on mRNA and POQR or negative on DNA. *BCR-ABL1* DNA negative and
571 mRNA POQR by qPCR was found in 25/674 samples (4%).
572 (B) Comparison of *BCR-ABL1*$_{RelDg}$ mRNA and DNA levels in CML patients using ddPCR (1279 samples
573 from 62 patients). The red line represents 100% concordance and dashed red lines delineate the area
574 of 95% confidence. By ddPCR, 366/1279 samples were quantifiable on both DNA and mRNA with 89%
575 of samples at levels ≥ 0.01% of *BCR-ABL1*$_{RelDg}$. ddPCR was negative for *BCR-ABL1* at both mRNA and
576 DNA level in 328/1279 samples. *BCR-ABL1* DNA quantifiable and mRNA POQR or negative was found
577 by ddPCR in 566 samples from remaining 585 samples. *BCR-ABL1* was by ddPCR DNA negative and
578 quantifiable or POQR on mRNA in 19/585 (3%) of samples.
579
580 **Figure 2. Correlation of the individual parameter estimates of mRNA and DNA *BCR-ABL1* samples**
581 **using the bi-exponential mixed effects models.** The first cohort of prospectively analysed CML
582 patients (n=81) with frequent monitoring during the first 6 months of TKI therapy (Supplementary
583 Table 1, Supplementary Figure 1A) were used to study whether DNA-based (*BCR-ABL1*$_{RelDg}$)
584 monitoring may be more precise and have greater predictive value during first months of TKI therapy
585 compared to mRNA-based (*BCR-ABL1*$_{RelDg}$) analysis. Validated DNA assays were achieved for 71/81
586 cases and samples for these 71 patients were analysed on the DNA and mRNA levels as follows; 64
587 patients were analysed by qPCR only and 7 patients were analysed by ddPCR only, because qPCR
588 analysis did not pass the quality criteria (reaction efficiency, correlation coefficient, slope). The
589 scatterplots show the estimated α slopes (left), B intercepts (middle) and β slopes (right) obtained
590 from either DNA and mRNA measurements of 67 patients (4 patients out of 71 with validated DNA

assays were excluded due to a quick TKI change after the start of first-line TKI treatment (n=1), a combination therapy with Interferon alpha (n=2) or higher than normal TKI doses (n=1)). The association of the estimated parameters between the two measurement methods are quantified by Pearson's correlation coefficient and visualized using linear regression.

Figure 3. Effects of co-variates on the individual parameter estimates of mRNA and DNA *BCR-ABL1* samples using the bi-exponential mixed effects models. Boxplots show the influence of the co-variates type of TKI (imatinib n=54 vs nilotinib n=13 (A), TKI dose (normal n= 29 vs reduced n= 38) (B) and transcript type (e13a2 n=27 vs e14a2 n= 40) (C) on the estimated individual α slopes (left) and β slopes (right) for both DNA based (blue) and mRNA based (green) measurements (*BCR-ABL1*$_{\text{RelDg}}$) of 67 patients from the first cohort (4 patients out of 71 of prospectively analysed patients (Table S1) with validated DNA assays were excluded due to a quick TKI change after the start of first-line TKI treatment (n=1), a combination therapy with Interferon alpha (n=2) or higher than normal TKI doses (n=1)) . P-values denote results of the Wald tests assessing the significance of the fixed effects.

Figure 4. Rates of DMR maintenance and molecular relapse after TKI cessation/interruption in 3 groups of patients that were divided according to DNA and mRNA *BCR-ABL1* $_{\text{RelDg}}$ **MRD pattern evaluated by the deterministic model in samples measured by ddPCR before TKI stop/interruption in EURO-SKI and INTReg patients.** The 3 groups are characterized based on a *BCR-ABL1* DNA and RNA status before TKI stop as follows: DNA positive/RNA positive (Red), DNA positive/RNA negative (Yellow) and DNA negative/RNA negative (Green). The pie graph that is portrayed as the traffic light shows the rate of DMR and molecular relapse after TKI stop/interruption in each patient's group. Measurements of *BCR-ABL1* at mRNA and DNA levels are illustrated by graphs of 3 example patients; a patient from the red group with molecular relapse after TKI interruption, a patient from the yellow group with molecular relapse after TKI interruption and a patient from the green group with sustained DMR after TKI cessation. The graphs show *BCR-ABL1* IS levels since diagnosis (black curve),

BCR-ABL1 positive samples on DNA level by ddPCR (dark blue filled circles) or negative (open dark blue circles) and *BCR-ABL1* positive samples on mRNA level by ddPCR (filled green circles) or negative (open green circles).

DMR – Deep Molecular Response; MolRel – Molecular Relapse; EURO-SKI – a patient from the EURO-SKI study; INTReg – patients with TKI interruption

Figure 5. Probability of molecular relapse-free survival after TKI cessation/interruption according to traffic light stratification model. Colours of curves indicate DNA and mRNA *BCR-ABL*1 pattern evaluated by deterministic model (Figure S6) using data from ddPCR measurement during DMR maintenance before TKI cessation or interruption; red=double positive, yellow=DNA positive/RNA negative; green= double negative.

Table 1 MRD evaluations of mRNA and DNA *BCR-ABL1* measurements by qPCR and ddPCR.

Assay	Negative	POQR	Quantifiable	Sensitivity
mRNA-qPCR*	Negative triplicates or averaged copies less than LoD (LoD=2.29 copies)	Averaged copies within the range LoD-LoQ (i.e. 2.29-7.64 copies)	Averaged number of copies equal or higher than LoQ (LoQ=7.64 copies)	At least 24 000 copies of control gene *GUSB* ensuring sensitivity MR4
mRNA-ddPCR	Negative quadruplicates or averaged copies less than LoD (LoD= 1.17 copies)	Averaged copies within the range LoD-LoQ (i.e. 1.17-3.95 copies)	Averaged number of copies equal or higher than LoQ (LoQ=3.95 copies)	
DNA-qPCR**	Negative triplicates or more than 4 Ct higher than the highest Ct of the individual calibration curve	Up to 4 Ct higher than the highest Ct of the individual calibration curve	Averaged Ct of triplicates within a quantification range specified by individual calibration curve	At least 20000 copies of control gene *ALB* (reflecting 10 000 cells) ensuring sensitivity 10^{-4}
DNA-ddPCR	Negative quadruplicates (no copy detected in negative controls of 6 healthy donors)***	NA	Averaged copy number (no copy detected in negative controls of 6 healthy donors)***	

** Conditions differ from the evaluation of deep MR recommended by ELN* [2] *to ensure reliable comparison with qPCR DNA analysis, which is a patient-specific.*

*** Conditions were applied as was previously described in Hovorkova et al.* [19].

**** All droplets observed after ddPCR DNA analysis of patient-specific assays were negative when 6 healthy donors were analysed.*

Abbreviations: LoD = Limit of Detection; LoQ = Limit of Quantification; ALB = albumin (ALB is recommended control gene for analysis of patient specific Ig/TCR rearrangement; standardized primers and probes were applied from EURO-MRD consortia [20]*), POQR = Positive Outside the Quantifiable Range*

Figure 1

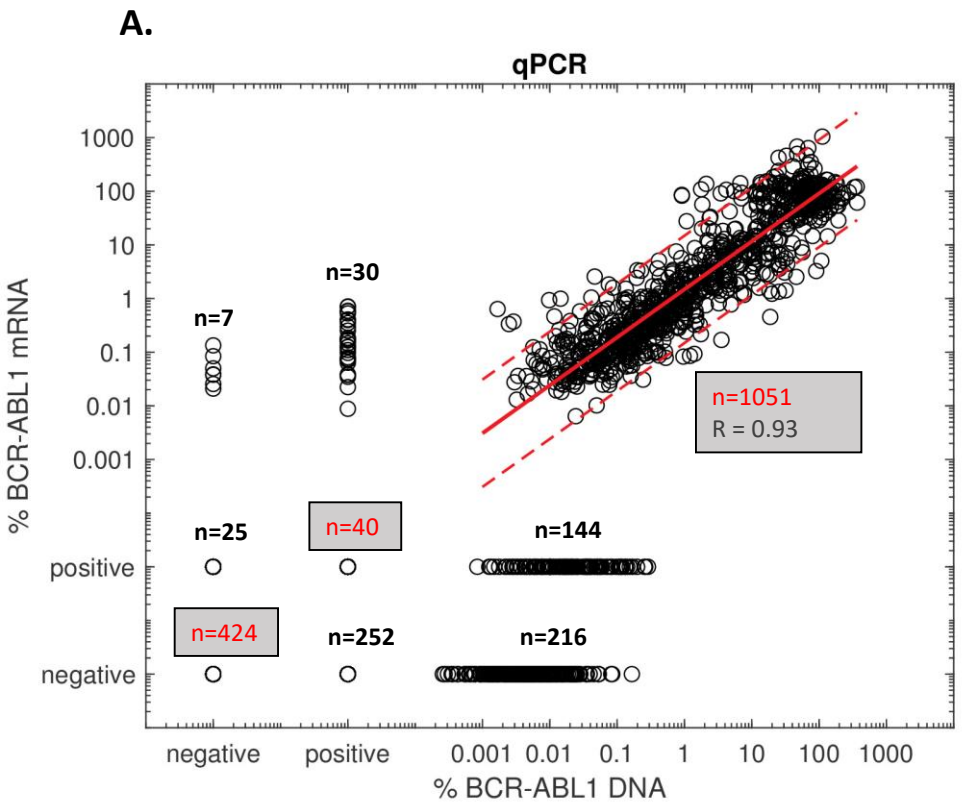

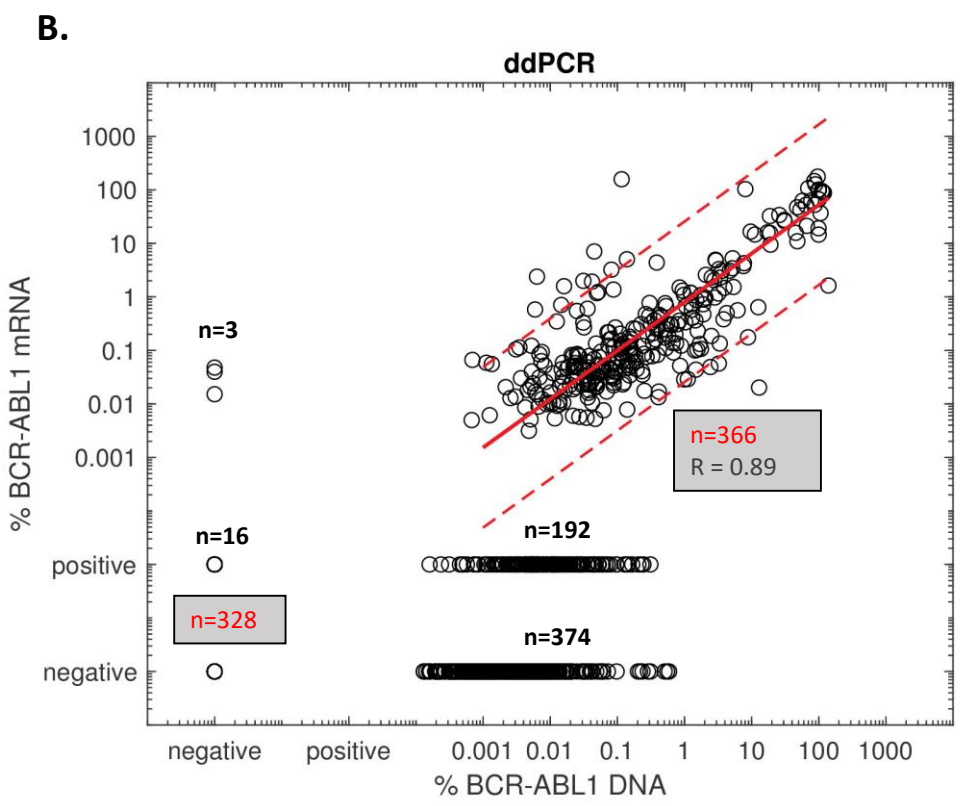

qPCR	RNA quantifiable	RNA POQR	RNA negative
DNA quantifiable	1051	144	216
DNA POQR	30	40	252
DNA negative	7	25	424

ddPCR	RNA quantifiable	RNA POQR	RNA negative
DNA quantifiable	366	192	374
DNA negative	3	16	328

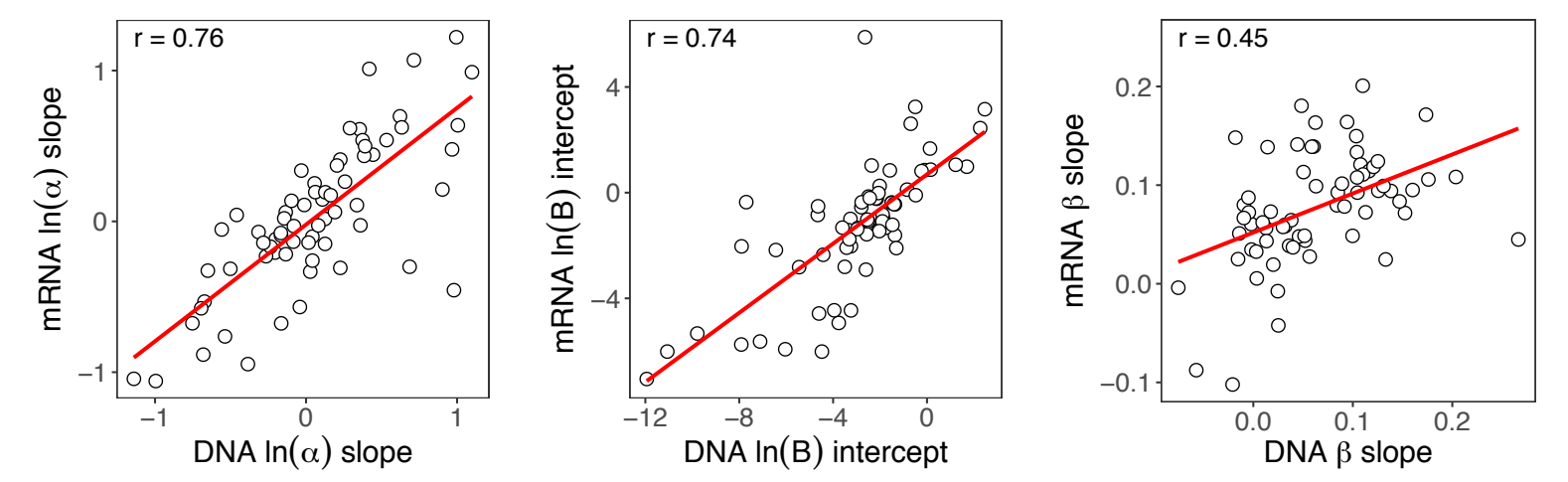
r = 0.76
mRNA ln(α) slope
DNA ln(α) slope
1
0
−1
−1
0
1
r = 0.74
mRNA ln(B) intercept
DNA ln(B) intercept
4
0
−4
−12
−8
−4
0
r = 0.45
mRNA β slope
DNA β slope
0.2
0.1
0.0
−0.1
0.0
0.1
0.2

Figure 4

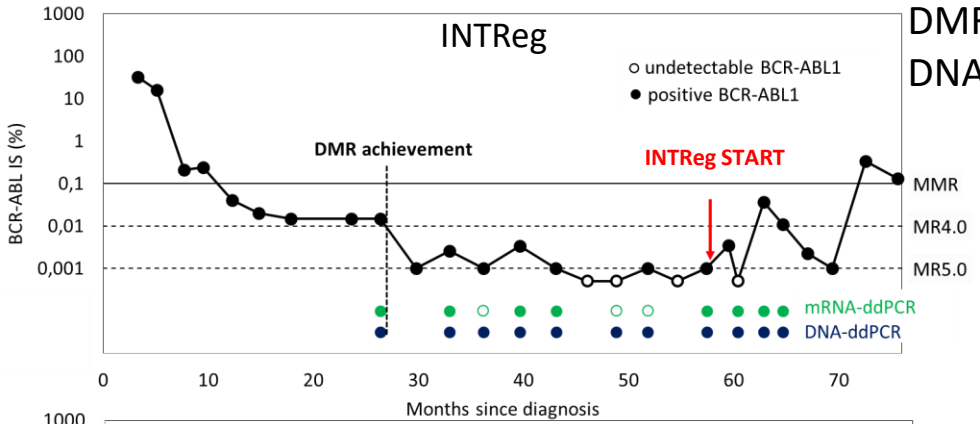

DMR pattern before TKI stop
DNApos/RNApos

EURO-SKI
N=17

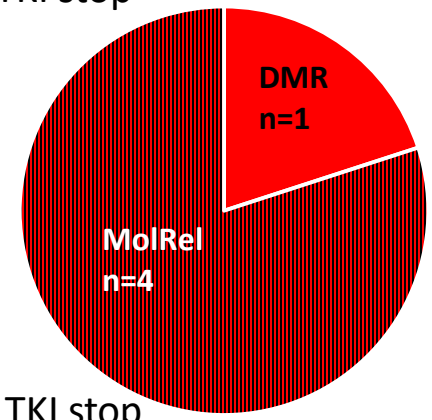

INTReg
N=25

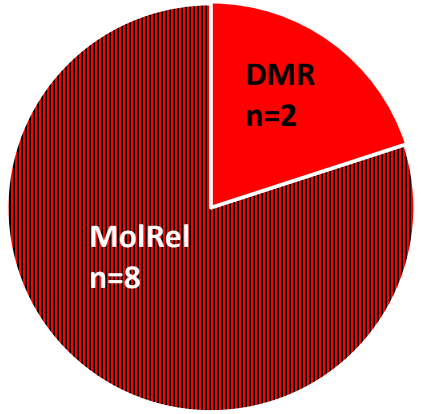

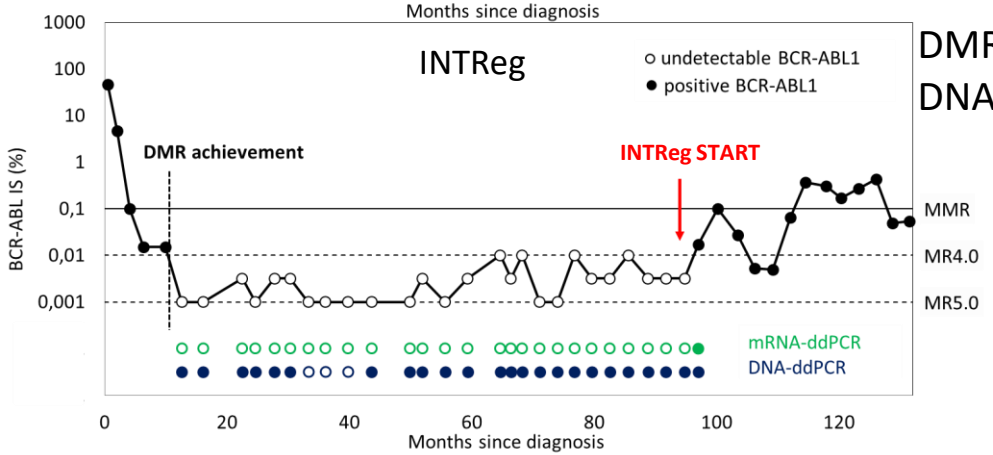

DMR pattern before TKI stop
DNApos/RNAneg

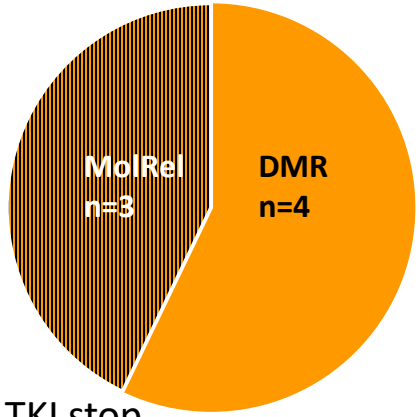

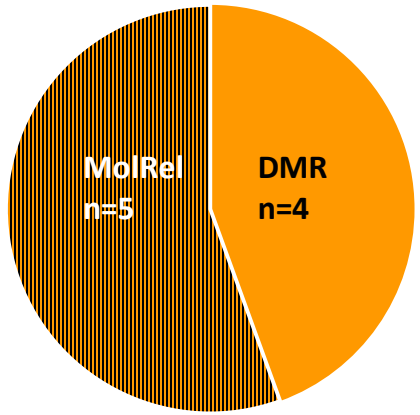

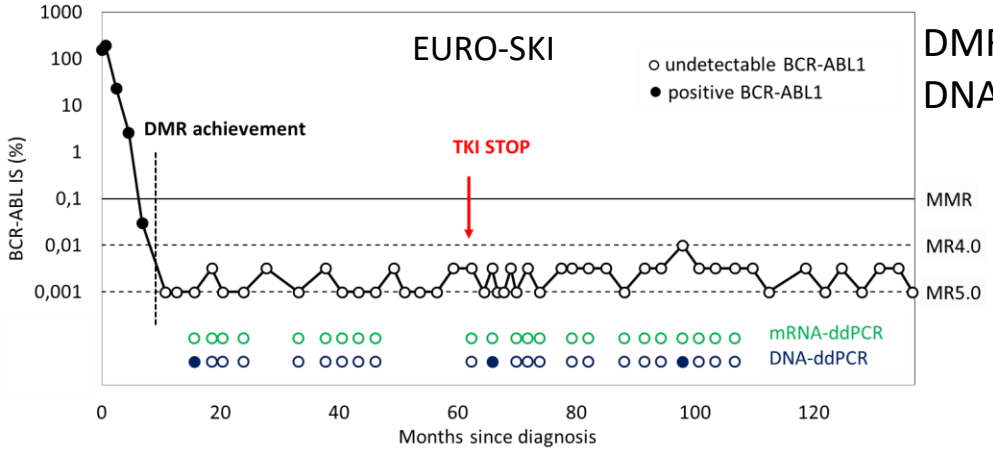

DMR pattern before TKI stop
DNAneg/RNAneg

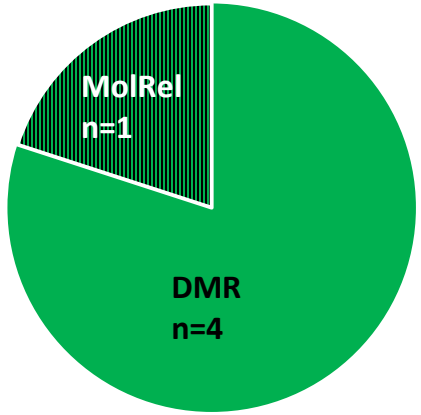

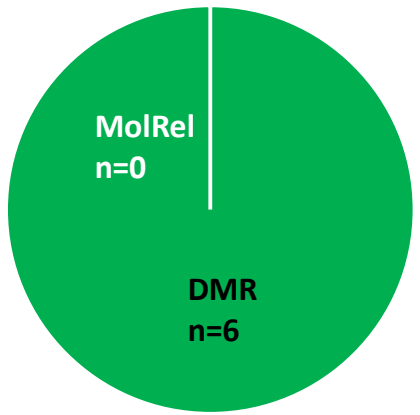

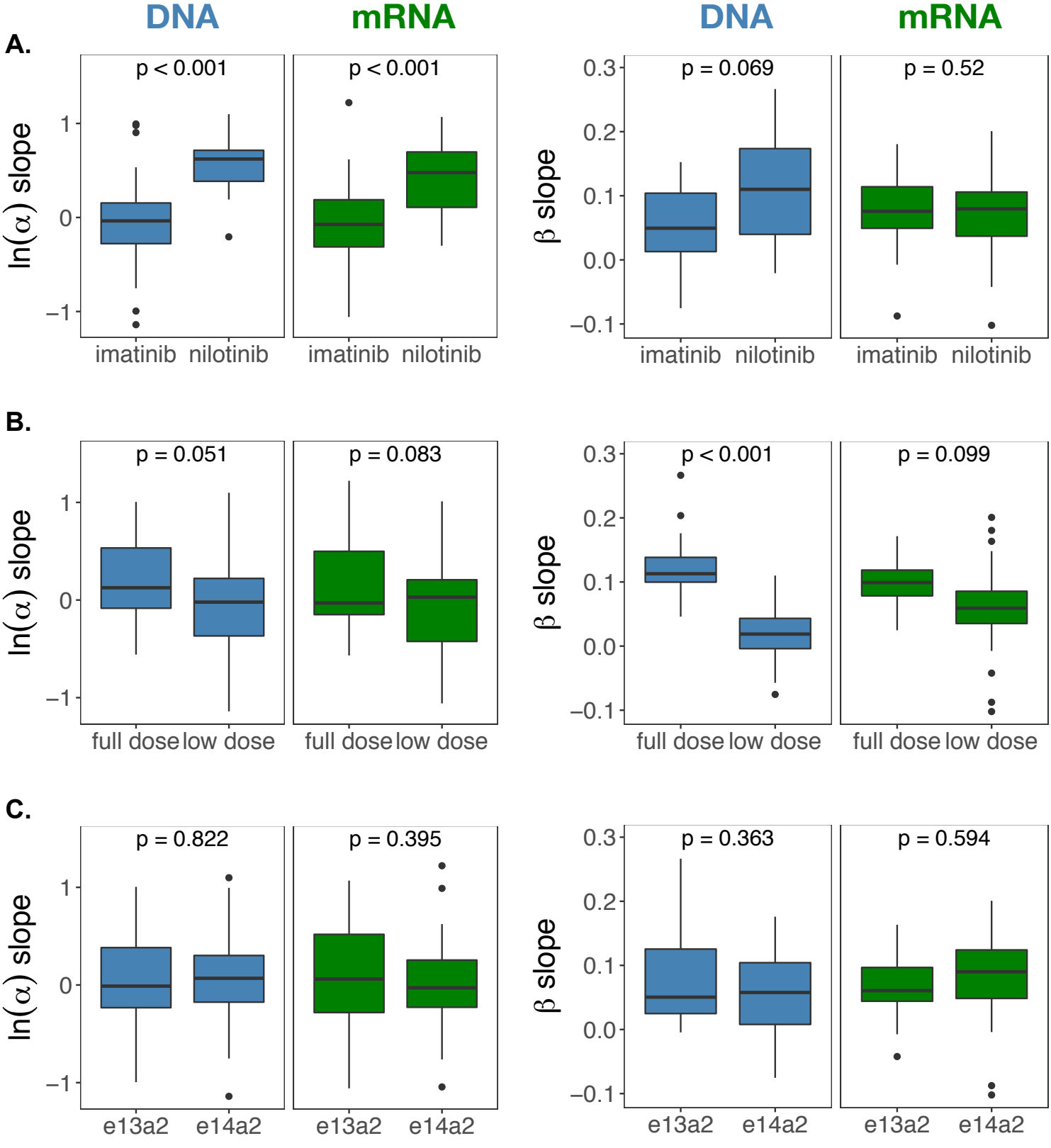
DNA
mRNA
DNA
mRNA
A.
p < 0.001
p < 0.001
p = 0.069
p = 0.52
ln(α) slope
β slope
imatinib
nilotinib
B.
p = 0.051
p = 0.083
p < 0.001
p = 0.099
full dose
low dose
C.
p = 0.822
p = 0.395
p = 0.363
p = 0.594
e13a2
e14a2

Figure 5

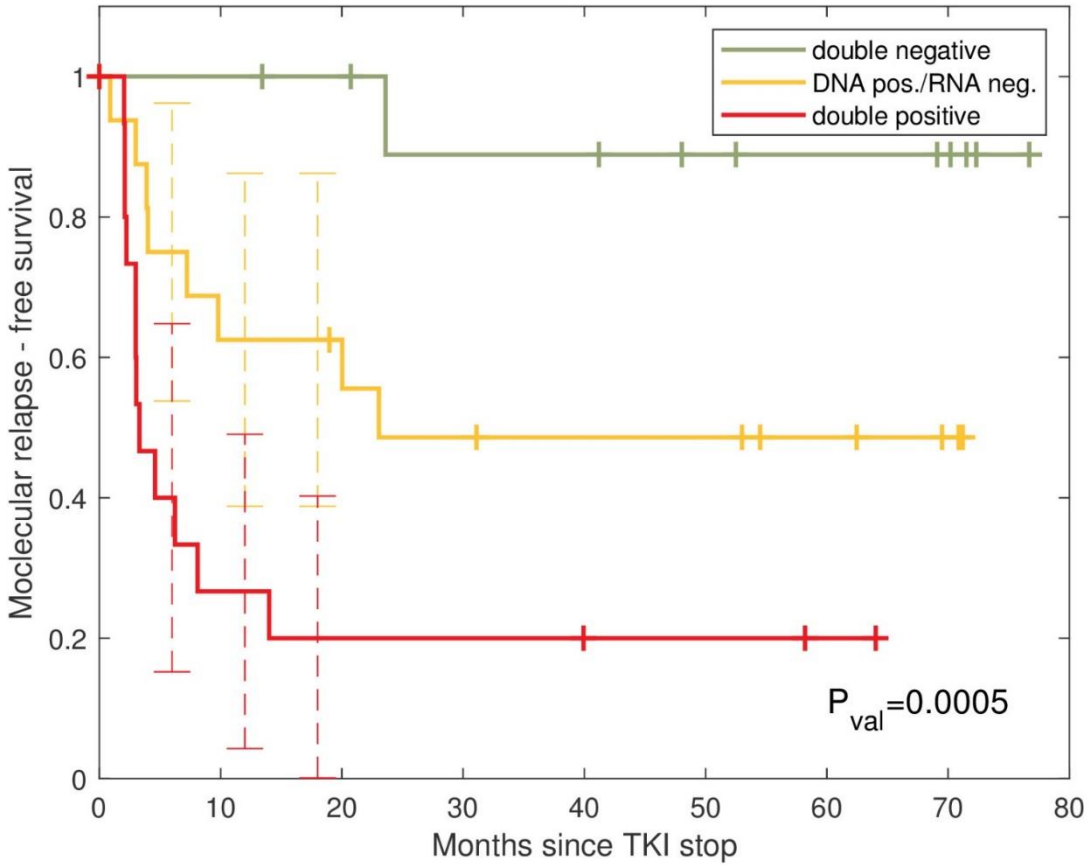

Cumulative number of relapse/censored patients	Months since TKI stop								
Number of patients=42	6	12	18	24	36	48	60	72	84
Double negative	0/0	0/0	0/1	1/2	1/2	1/3	1/5	1/8	1/10
DNA positive / RNA negative	4/0	6/0	6/0	8/1	8/2	8/2	8/4	8/8	8/8
Double positive	9/0	11/0	12/0	12/0	12/0	12/1	12/2	12/3	12/3

Supplementary Materials and Methods

The detailed version of the Materials and Methods of the Article "Analysis of chronic myeloid leukemia during deep molecular response by genomic PCR: a traffic light stratification model with impact on treatment-free remission" by Machova Polakova et al.

Patient cohorts

The first cohort consisted of 81 newly diagnosed CML patients enrolled within the years 2016-2018 (Table S1) who had given their consent for frequent visits during the first 6 months of TKI therapy according to the time schedule shown in Figure S1A. Forty-eight patients were referred to the Institute of Hematology and Blood Transfusion Prague, and 33 patients were referred to the Internal Hematology and Oncology Clinic, Faculty Hospital Brno. This cohort allowed to study whether DNA-based *BCR-ABL1* measurements during the first months since the start of TKI therapy may be a useful parameter for early molecular response (EMR) measurements compared to measurements at the transcript level. In all patients from the first cohort (n=81), the *BCR-ABL1* genomic fusions were successfully characterized.

The second cohort consisted of 87 patients who achieved and maintained DMR during long-term treatment at the Institute of Hematology and Blood Transfusion, Prague. The breakpoints could not be characterized in 10/87 cases (primarily due to unavailability of suitable DNA, however we cannot exclude that in some cases a cause of a failure of a BCR-ABL1 genomic fusion characterisation may be a presence of a breakpoint in a repetitive sequence that is difficult to amplify or to sequence), leaving 77 for analysis. The clinical and biological characteristics (age, response to TKI, duration of TKI treatment) of the 10 patients did not differ from the 77 included cases (Table S2). This cohort of patients allowed to investigate differences in measurable residual disease (MRD) at the DNA and mRNA levels (Figure 1SB). Of these 77 patients, 35 continued with TKI therapy, while 17 were included in the EURO-SKI study and ceased treatment. The remaining 25 patients, who fulfilled the cessation criteria but could not be involved in the EURO-SKI trial, gave consent for an intermittent regimen (INTReg) of TKI administration every second month. The molecular relapse-free survival (MRFS) rate of INTReg patients was comparable to that reported in the EURO-SKI at later time points (48% at 24 months; Figure S2) [1]. In the case of MMR loss (n=13), a full dose of TKIs was reintroduced by every day TKI consumption. All 13 patients re-achieved DMR. In one patient the TKI therapy was completely withdraw after 30 months of TKI reintroduction in full dose, and remains in DMR for 36 months. One patient died from myocardial infarction. Twelve patients with sustained DMR remained on TKI administration every second month for median 20 months since INTReg start (range 13-86 months). The therapy was completely stopped in one patient after 58 months in DMR

on INTReg therapy and sustained DMR for 12 months up to now. Two patients died from colon cancer and myocardial infarction.

Patient-specific genomic *BCR-ABL1* fusion characterization

Patient-specific DNA *BCR-ABL1* fusions were characterized in 158 (81 + 77) patients from both cohorts using two approaches. The first approach was based on long-distance PCR (LD-PCR) and was described previously [2]. The second approach was based on next-generation sequencing (NGS) technology using the Illumina platform and the Rapid Capture Custom Enrichment approach (Illumina, San Diego, CA, USA), which includes 4608 probes covering genomic regions of the *BCR* gene (chr. 22; 23522352-23660424) and the *ABL*1 gene (chr. 9; 133589068-133763262), including upstream and downstream regions of both genes. The manufacturers' protocols were followed for sample and library preparation. MiSeq Reagent Kit v3 was used for sequencing performance (Illumina). The observed reads in fastq format were evaluated using NextGENe software (Softgenetics, State College, PA, USA).

Real-time qPCR (qPCR)

DNA and RNA were extracted from the same amount of white blood cells (5-20x10^6) isolated from the peripheral blood and bone marrow samples.

DNA qPCR

The theoretical yield of DNA from 10x10^6 cells is 66,000 ng DNA (6.6 pg per cell). The optimal concentration of total DNA for qPCR is 100 ng/µl (1000 ng/analysis). The minimal required DNA concentration was estimated to be 6.6 ng/µl, which corresponds to the requested minimal sensitivity of 10^{-4} (one leukaemic cell/10,000 cells) if 10 µl of DNA is added to the qPCR. The sensitivity of each qPCR analysis was determined by the total amount of DNA present in the qPCR as follows:

- sensitivity 10^{-4}; 66 ng – 660 ng of DNA (i.e., 10^4 – 10^5 cells)
- sensitivity 10^{-5}; 660 ng – 6600 ng of DNA (i.e., 10^5 – 10^6 cells).

The median amount of DNA in 10 µl analysed by qPCR from 1794 samples was 967.3 ng (75.5-4863.4 ng).

Patient-specific primers and TaqMan probes were designed using the PrimerQuest Tool (Integrated DNA Technologies, Coralville, Iowa, USA). qPCR efficiency was initially tested for each patient-specific assay. Primers and probes were designed and passed PCR quality criteria for 148 of 158 patient-specific *BCR-ABL1* fusions. The ten patients for whom adequate qPCR could not be designed were all from the first cohort of prospectively analysed CML patients.

The rules for patient-specific DNA qPCR analysis were adopted from the recommendation of the EURO-MRD consortia for patient-specific Ig/TCR rearrangement analysis. According to the recommendation, the albumin (*ALB*) gene was applied as a control gene with standardized primers and probes [3]. A calibration curve for *ALB* quantification was created based on the dilution of human genomic DNA with a known concentration of 200 ng/µl (Roche). The recommended dilution range was 200 ng/µl (10^0) – 0.2 ng/µl (10^{-3}).

The total DNA concentration was calculated from the duplicate analysis of *ALB*. The Ct values of the duplicates did not differ more than one cycle up to the 30th cycle and no more than two cycles after the 30th cycle of the qPCR.

Of 148 patient-specific assays, 19 did not pass quality criteria (reaction efficiency, correlation coefficient, slope – see below) for qPCR analysis. These were successfully analysed by droplet digital PCR (ddPCR) only thus enabling quantitative analysis for all cases. Copy number analysis of individual *BCR-ABL1* genomic fusions by qPCR (n=129) was performed using the calibration curves calculated from the DNA sample of each individual patient collected at the time of diagnosis (n=82/129, median 35% *BCR-ABL1* on the IS; range 5-140%; Table 1). In patients where the diagnostic sample was not available (n=47/129 patients from the second cohort only), the first available sample with the highest *BCR-ABL1* IS level (median 34% *BCR-ABL1* on the IS; range 0.52-66%, Table 2) was used for creating the calibration curve dilutions and considered as a sample with 100% level. Thus, in the Article, for the comparisons of mRNA vs. DNA *BCR-ABL1* levels, these samples are also assigned as diagnostic.

First, the DNA concentration was measured at the time of diagnosis using the control gene ALB. If the concentration of the sample at diagnosis was too low (<100 ng/ul), the starting sample for dilutions was adjusted to 10 ng/µl (10^{-1}). The calibrators were then prepared by decimal dilutions of the starting DNA with DNA from a healthy donor, which had the same concentration as the starting DNA of a patient. Prepared patient-specific calibration standards 10^{-1}-10^{-3} were analysed in duplicate, and those 10^{-4} and 10^{-5} were analysed in triplicate.

Each qPCR for patient-specific genomic *BCR-ABL1* (*gBCR-ABL1*) fusion assays and for *ALB* quantification met the following criteria:

- reaction efficiency range 95-100%
- correlation coefficient of the calibration curve ≥ 0.98
- slope range from -3.1 to -3.9.

As negative controls, we used DNAs from 6 different healthy donors analysed as single reactions or DNA samples from 3 healthy donors analysed in duplicate. Patient samples with *BCR-ABL1* transcripts > 0.01% IS (known from the routine *BCR-ABL1* mRNA transcript monitoring) were measured in duplicate, and patient samples with *BCR-ABL1* transcripts < 0.01% IS were measured in triplicate.

mRNA qPCR

BCR-ABL1 qPCR at the transcript level was performed using *GUSB* as a control gene and with primers and probes that are used for standardized monitoring on the IS [4]. Certified ERM-AD623 (Sigma-Aldrich, St Louis, MO, USA) standards were used to determine the copy numbers of *BCR-ABL1* and *GUSB*. In each qPCR run, 2 negative (healthy donor and no template control) and 2 positive controls (samples with 1% and 0.01% *BCR-ABL1* IS prepared from K562 cell line) were analysed. Patient samples with *BCR-ABL1* transcripts > 0.01% IS were measured in duplicate, and patient samples with *BCR-ABL1* transcripts < 0.01% IS were measured in triplicate. The *BCR-ABL1* level on the IS was determined from the standardized monitoring of *BCR-ABL1* for clinical practice that preceded the mRNA and DNA measurements applied in this study.

The median total copy number of *GUSB* analysed by qPCR from 2788 samples was 157831 (48020-1793119). The copy number 24000 of *GUSB* corresponds to MR4, 77000 to MR4.5 and 240000 to MR5 [4].

Droplet digital PCR (ddPCR)

ddPCR was performed using the QX200 AutoDG Droplet Digital (Bio-Rad, Hercules, CA, USA). The maximum concentration of DNA allowed to perform ddPCR was 100 ng/µl (a higher concentration of DNA overloaded the system and did not allow the quantification of *BCR-ABL1*). Each patient-specific assay was tested to find the optimal annealing temperature using a gradient of 50°C-60°C. The reaction mixture preparation and conditions were applied according to the recommendations of the manufacturer (BioRad). Patient samples were analysed in quadruplicate. Six negative controls (healthy donors) were applied for each patient-specific assay. Samples with <10 000 droplets were discarded from the analysis. The sensitivity of the analysis was determined by the copy numbers of *ALB*: 20 000 copies = 10^{-4}; 200 000 copies = 10^{-5}; and 2 000 000 copies = 10^{-6}.

ddPCR analysis of *BCR-ABL1* transcripts was performed using the primers and probes used for qPCR. The copy number of *GUSB* was analysed by qPCR due to the high expression of *GUSB*, which exceeds the limit allowed for ddPCR analysis. Samples were analysed in quadruplicate. Each ddPCR run included 2 positive controls, 1 negative control (healthy donor) and a non-template control (NTC). The reaction mixture preparation and conditions were applied according to the manufacturer's recommendations (BioRad).

The Limit of Blank (LoB), Limit of Detection (LoD) and Limit of Quantification (LoQ) calculation for mRNA analysis by qPCR and ddPCR

Peripheral blood samples of 45 healthy donors (8 females and 37 males; median age 39 years, range 24-60) were applied for LoB analysis. *BCR-ABL1* mRNA measurement by qPCR in duplicates in all 45

tested samples were negative (median copy number of *GUSB* 340 793, range 100 059 – 569 070). BCR-ABL1 mRNA detection by ddPCR in 45 healthy donors showed 1 positive droplet detected in one of 4 replicates in 2 samples resulting in LoB=0.175 copy.

BCR-ABL1 positive sample from CML patient was used to prepare 6 diluted samples with expected copy number of mRNA *BCR-ABL1* 24, 12, 6, 3, 1.5, 0.75 for LoD and LoQ estimation. LoD of mRNA *BCR-ABL1* measurement by qPCR and ddPCR was 2.29 copies and 1.17 copies, respectively. LoQs were 7.64 by qPCR and 3.95 by ddPCR.

DNA and mRNA *BCR-ABL1* data evaluations

The first cohort of prospectively analysed CML patients (n=81) with frequent monitoring during the first 6 months of TKI therapy (Table S1, Figure S1A) were used to study whether DNA-based monitoring may be more precise and have greater predictive value during first months of TKI therapy compared to mRNA-based analysis. Validated DNA assays were achieved for 71/81 cases and samples for these 71 patients were analysed on the DNA and mRNA levels as follows; 64 patients were analysed by qPCR only and 7 patients were analysed by ddPCR only, because qPCR analysis did not pass the quality criteria (reaction efficiency, correlation coefficient, slope). Patients with long term DMR during TKI therapy from the second cohort (n=77; Table S2, figure S1B) were used to compare the precision and sensitivity of DNA vs mRNA analysis of MRD in 65 patients by qPCR and 12 patients by ddPCR only (due to poor qPCR quality). For 43/65 patients tested by qPCR, sufficient mRNA and DNA was available to perform ddPCR for MRD measurements and thus enabling a direct comparison with qPCR.

The quantity of *gBCR-ABL1* (genomic *BCR-ABL1*) from qPCR analysis was determined in relation to the corresponding quantity in the diagnostic sample (the level of *gBCR-ABL1* in this sample was defined as 100%) using the following calculations:

1) % *gBCR-ABL1*= (⌀ concentration *BCR-ABL1* DNA)/(⌀ concentration of total DNA (*ALB*))*100

2) % $gBCR\text{-}ABL1_{RelDg}$= (% $gBCR\text{-}ABL1_{sample}$)/(% $gBCR\text{-}ABL1_{Dg}$)*100.

Although ddPCR provides an absolute quantification, the results were related to the quantity of the diagnostic sample for the reliable comparison of qPCR and ddPCR approaches. The quotations used for ddPCR data evaluations were as follows:

1) % *gBCR-ABL1* sample= (⌀ copy number of *gBCR-ABL1*)/(⌀ copy number of *ALB*)*100

2) % $gBCR\text{-}ABL1_{RelDg}$= (% $gBCR\text{-}ABL1_{sample}$)/(% $gBCR\text{-}ABL1_{Dg}$)*100.

For the reliable comparison of mRNA and DNA *BCR-ABL1* data, mRNA *BCR-ABL1* data from qPCR and ddPCR measurements were also related to the level of the diagnostic sample, which was defined as 100%.

Stringent quality requirements were established to exclude poor-quality samples from the evaluations (Article - Table 1).

Statistical analysis

First-line TKI therapy in responding CML patients typically induces a biphasic decline in *BCR-ABL1* levels, which is (on the log-scale) characterized by an initially steep decline (to which we refer to as the α slope, starting at intercept A) followed by a second moderate decline (referred to as the β slope, starting at intercept B) [5]. Technically, all *BCR-ABL1* levels are log-transformed: log10(% *gBCR-ABL1*$_{RelDg}$) for DNA measurements or log10(% *BCR-ABL1*$_{RelDg}$) for mRNA. Negative *BCR-ABL1* levels and positive *BCR-ABL1* levels outside the quantifiable range (POQR) were treated as left-censored observations with global or individual upper quantification limits (QL) at DNA or mRNA level, respectively. The upper quantification limit of negative *BCR-ABL1* levels was estimated by

- negative QL_{DNA} = log10((0.00001%)/(% *gBCR-ABL1*$_{Dg}$)*100) or
- negative QL_{mRNA} = log10((3/measurement of control gene*100)/(% *BCR-ABL1*$_{Dg}$)*100),

whereas, the upper quantification limit of POQR *BCR-ABL1* levels was estimated by

- POQR QL_{DNA} = log10((0.0001%)/(% *gBCR-ABL1*$_{Dg}$)*100) or
- POQR QL_{mRNA} = log10((10/measurement of control gene*100)/(% *BCR-ABL1*$_{Dg}$)*100)

at DNA or mRNA level, respectively.

We further included the *type of TKI* (levels: imatinib vs. nilotinib), *TKI dose* (levels: full dose (i.e. 400 mg imatinib or 600 mg nilotinib) vs. low dose) and the *transcript type* (levels: e13a2 vs. e14a2) as additional covariates in the bi-exponential mixed effect models, in which they were represented as fixed effects of the α and β slopes, assuming the same model structure as published in Glauche 2018. We applied Wald tests to assess the statistical significance of the fixed effect group effects. For model fitting and evaluation, we applied the software "Monolix" (version 2018R2) (lixoft.com/products/monolix/). The correlation of the estimated parameters between DNA-based and mRNA-based measurements was quantified using Pearson's correlation coefficient.

The cumulative incidences of molecular relapse free survival after TKI stop/interruption were depicted using the Kaplan-Meier method. All the curves are presented with 95% confidence intervals (CIs). Differences in cumulative incidences between patient groups were assessed using the log-rank test. The follow-up was defined from the date of treatment cessation (TKI cessation) to the date of molecular relapse or the end of follow-up (1 May 2019), whichever came first. An event was defined as the occurrence of molecular relapse. The Cox regression analysis was used to estimate the effect of duration of TKI, duration of DMR and transcript type (e13a2 vs. e14a2) on molecular relapse free survival. All tests were two-sided, as the analyses were considered exploratory, and no correction for

multiple testing was performed. To statistically demonstrate the superiority of DNA and/or RNA *BCR-ABL1* for TFR prediction, the Cox model was fitted using a forward stepwise variable selection process. The deterministic model to identify patterns of DNA and RNA results during DMR before TKI stop/interruption was developed using INTReg data and validated using EURO-SKI data. For all analyses, p-values<0.05 were considered statistically significant.

Statistical analysis was performed using the statistical programming environment R (R Core Team (2018). R: A language and environment for statistical computing. R Foundation for Statistical Computing, Vienna, Austria. URL https://www.R-project.org/.) and MATLAB version R2019b.

References:

1. Saussele S, Richter J, Guilhot J, Gruber FX, Hjorth-Hansen H, Almeida A, et al. Discontinuation of tyrosine kinase inhibitor therapy in chronic myeloid leukaemia (EURO-SKI): a prespecified interim analysis of a prospective, multicentre, non-randomised, trial. Lancet Oncol. 2018;19:747-757.
2. Hovorkova L, Zaliova M, Venn NC, Bleckmann K, Trkova M, Potuckova E, et al. Monitoring of childhood ALL using *BCR-ABL1* genomic breakpoints identifies a subgroup with CML-like biology. Blood. 2017;129:2771-2781.
3. van der Velden VH, Cazzaniga G, Schrauder A, Hancock J, Bader P, Panzer-Grumayer ER, et al. Analysis of minimal residual disease by Ig/TCR gene rearrangements: guidelines for interpretation of real-time quantitative PCR data. Leukemia. 2007;21:604-611.
4. Cross NC, White HE, Müller MC, Saglio G, Hochhaus A. Standardized definitions of molecular response in chronic myeloid leukemia. Leukemia. 2012;26(10): 2172-5.
5. Glauche I, Kuhn M, Baldow C, Schulze P, Rothe T, Liebscher H, et al. Quantitative prediction of long-term molecular response in TKI-treated CML - Lessons from an imatinib versus dasatinib comparison. Sci Rep. 2018. 8:12330.

Table 1. Level of *BCR-ABL1* at the time of diagnosis on the IS in 81/129 patients used for calibration curve creation for DNA analysis and was considered as 100% for DNA and also mRNA data evaluation.

Patients	***BCR-ABL1* % IS**	**Patients**	***BCR-ABL1* % IS**	**Patients**	***BCR-ABL1* % IS**	**Patients**	***BCR-ABL1* % IS**
AZV-N-P55	5	AZV-I-P57	27	AZV-N-B139	36	AZV-N-B165	53
AZV-E-P7	6	AZV-E-P2	27	AZV-N-P46	37	AZV-N-P59	55
AZV-I-P122	9	AZV-E-P11	28	AZV-N-B161	38	AZV-N-B142	55
AZV-E-P34	12	AZV-I-P35	29	AZV-N-B149	35	AZV-E-P61	57
AZV-E-P27	15	AZV-E-P118	29	AZV-N-P103	40	AZV-N-P50	58
AZV-N-P75	16	AZV-N-P6	29	AZV-N-B135	40	AZV-N-P99	59
AZV-N-P117	16	AZV-S-P58	30	AZV-N-P73	42	AZV-E-P29	61
AZV-N-B152	18	AZV-E-P124	30	AZV-E-P9	43	AZV-E-P5	64
AZV-N-P119	18	AZV-N-P78	30	AZV-N-B172	44	AZV-E-P17	66
AZV-I-P31	20	AZV-N-B170	30	AZV-N-B153	45	AZV-N-P85	67
AZV-S-133	21	AZV-I-P24	31	AZV-N-P47	46	AZV-N-P110	68
AZV-N-B151	22	AZV-S-P112	32	AZV-N-P68	46	AZV-N-P111	77
AZV-N-B160	22	AZV-E-P13	32	AZV-N-P80	48	AZV-E-P100	84
AZV-E-P12	23	AZV-N-B171	33	AZV-E-P45	49	AZV-N-B138	84
AZV-N-P30	23	AZV-N-P28	34	AZV-N-P101	50	AZV-N-P66	85
AZV-N-P81	23	AZV-N-P114	34	AZV-N-P82	50	AZV-N-P97	92
AZV-S-P83	24	AZV-N-P115	34	AZV-N-B163	51	AZV-I-P107	95
AZV-N-P48	24	AZV-N-P116	34	AZV-N-B175	52	AZV-N-B148	102
AZV-E-P60	25	AZV-N-P130	34	AZV-N-P33	53	AZV-I-P32	140
AZV-N-B136	25	AZV-N-P88	35	AZV-N-P71	53		
AZV-N-P96	26	AZV-E-P25	36	AZV-N-B144	53		

Table 2. Level of *BCR-ABL1* on the IS in the first available sample with the highest *BCR-ABL1* IS level in 47/129 patients. These samples were used for creating the calibration curve dilutions and considered as a sample with 100% level for DNA and also mRNA data evaluation.

Patients	***BCR-ABL1* % IS**	**Patients**	***BCR-ABL1* % IS**	**Patients**	***BCR-ABL1* % IS**	**Patients**	***BCR-ABL1* % IS**
AZV-S-P79	0.52	AZV-S-P18	22	AZV-E-P42	36	AZV-N-B146	44
AZV-E-P104	9	AZV-N-P38	22	AZV-E-P125	36	AZV-E-P82	45
AZV-N-P26	9	AZV-S-P64	25	AZV-N-B164	36	AZV-S-P23	47
AZV-I-P95	9	AZV-I-P62	27	AZV-I-P3	37	AZV-N-B155	47
AZV-N-P98	10	AZV-E-P94	27	AZV-E-P20	37	AZV-E-P123	52
AZV-S-P21	15	AZV-E-P22	27	AZV-E-P53	38	AZV-E-P16	52
AZV-S-P93	15	AZV-E-P67	29	AZV-I-P37	38	AZV-E-P90	57
AZV-E-P65	17	AZV-N-B173	29	AZV-N-B174	39	AZV-N-B143	58
AZV-E-P52	20	AZV-E-P91	30	AZV-E-P131	40	AZV-E-P40	59
AZV-E-P19	21	AZV-E-P77	31	AZV-E-P121	40	AZV-E-P72	64
AZV-S-P51	21	AZV-E-P106	31	AZV-S-P92	41	AZV-E-P132	66
AZV-N-P102	21	AZV-E-P70	34	AZV-N-B141	44		

Figure S1. Frequency of *BCR-ABL1* monitoring and duration of TKI treatment of CML patients. (A) The cohort of *de novo* CML patients (n=81, Table S1) analysed prospectively with more frequent monitoring during first six months since TKI start and (B) and the cohort of CML patients (n=77, Table S2) with long-term TKI treatment and DMR maintenance. The black arrows outline the sampling schedule for DNA based measurements in the early phase of TKI therapy (A) and the effectiveness of DNA based MRD (B), respectively.

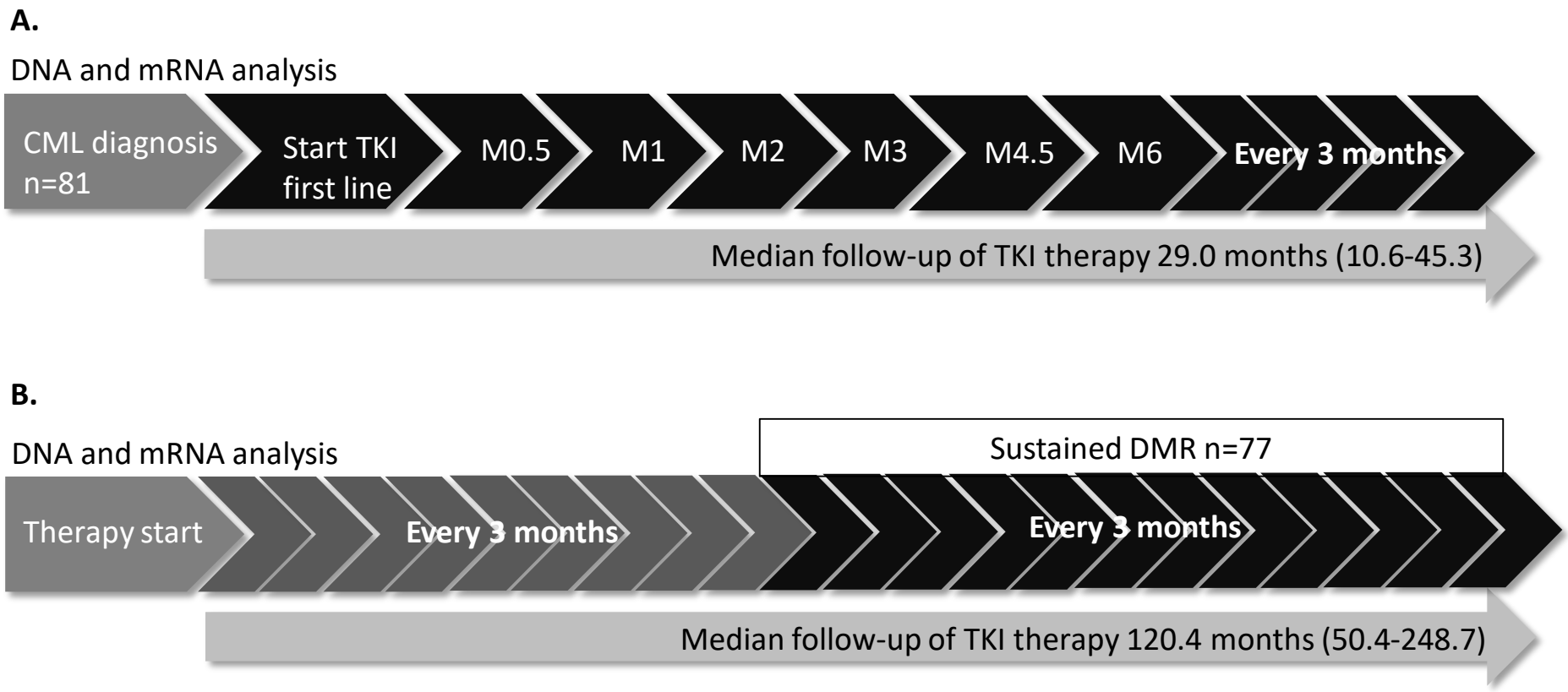

Figure S2. The probability of molecular relapse-free survival in CML patients after TKI administration every second month.
INTReg – intermittent regimen of TKI administration in 25 patients

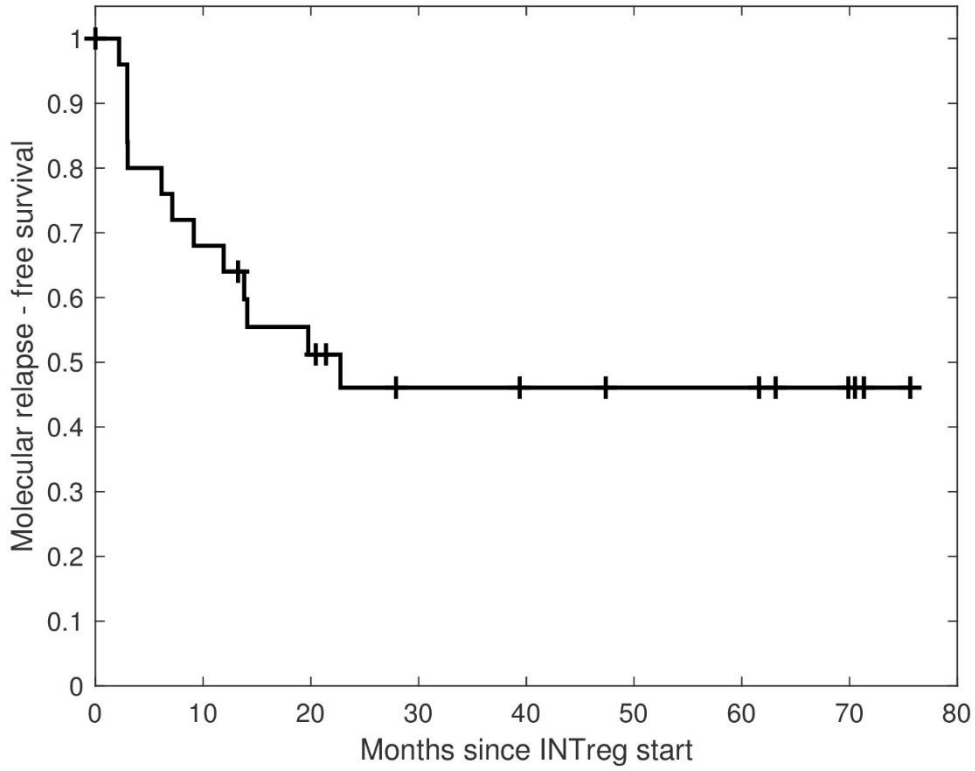

Cumulative number of relapse/censored patients									
Number of patients=25	Months since TKI interruption								
	6	12	18	24	36	48	60	72	84
Intermittent	5/0	9/0	11/1	13/3	13/4	13/6	13/6	13/11	13/12

Figure S3. Comparison of *BCR-ABL1*$_{RelDg}$ data at mRNA and DNA levels. (A) and (B) show the number of *BCR-ABL1* positive samples after both DNA and mRNA measurements in 128 patients by qPCR and in 61 patients by ddPCR. Black dots indicate the number of *BCR-ABL1* DNA and mRNA positive samples in one patient. Coloured dots show the number of *BCR-ABL1* positive samples on DNA and mRNA level found in more than one patient. POQR – positive outside quantifiable range

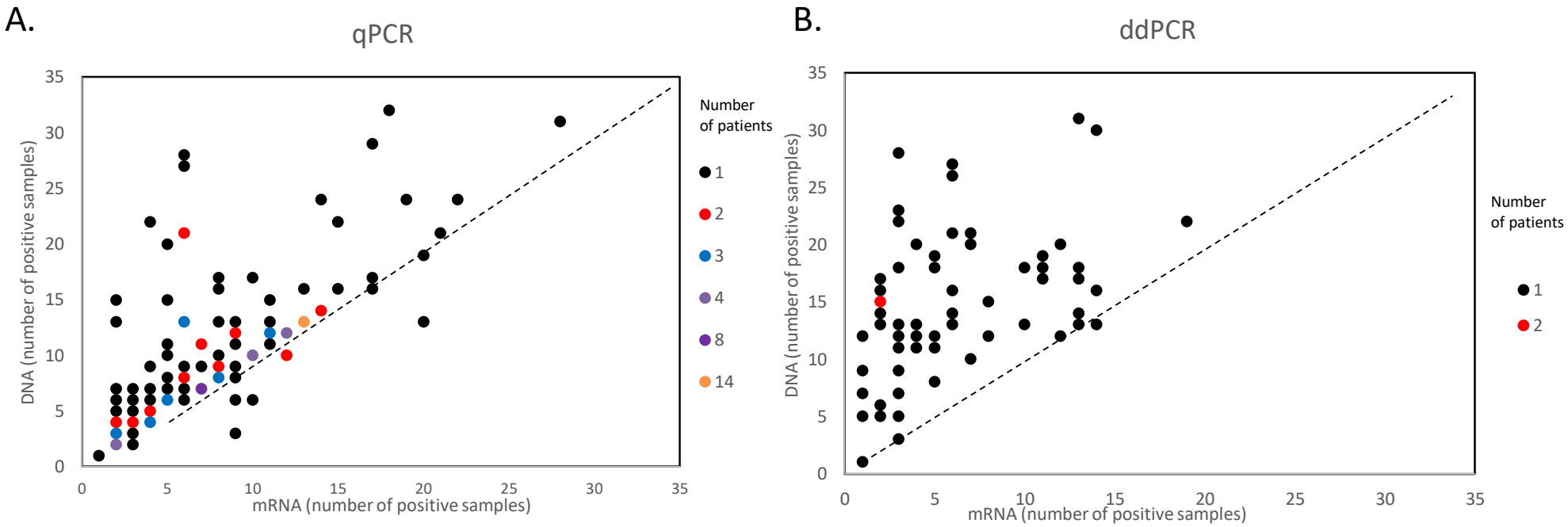

Figure S4. Comparison of ddPCR and qPCR for measurement of *BCR-ABL1* at the mRNA and DNA levels. (A) ddPCR and qPCR were compared at the mRNA level in 1032 samples from 43 patients. The red line represents 100% concordance and dashed red lines delineate the area of 95% confidence. Of the 1032 results, 846 (82%) results were considered concordant, i.e. both techniques yielded quantifiable *BCR-ABL1* (n=191; r=0.98), POQR (n=64) or undetectable *BCR-ABL1* (n=591). Of the remaining 186 samples that were discordant, quantifiable *BCR-ABL1* was detected by ddPCR that were POQR or negative by qPCR (n=66); ddPCR resulted in POQR *BCR-ABL1* that were by qPCR negative (n=107); *BCR-ABL1* was quantifiable by qPCR that were POQR or negative by ddPCR (n=4) or *BCR-ABL1* was POQR by qPCR but undetectable by ddPCR (n=9). (B) ddPCR and qPCR were compared at the DNA level in 864 samples from the same 43 patients. Of these 864 samples, 539 (62%) were concordant with *BCR-ABL1* detected and quantifiable by both techniques (n=368; r=0.96) or negative by both techniques (n=171). Of the 325 discordant samples, *BCR-ABL1* was quantifiable by ddPCR that were POQR or negative by qPCR-DNA (n=282) or *BCR-ABL1* was by quantifiable or POQR by qPCR but *BCR-ABL1* negative by ddPCR (n=43).

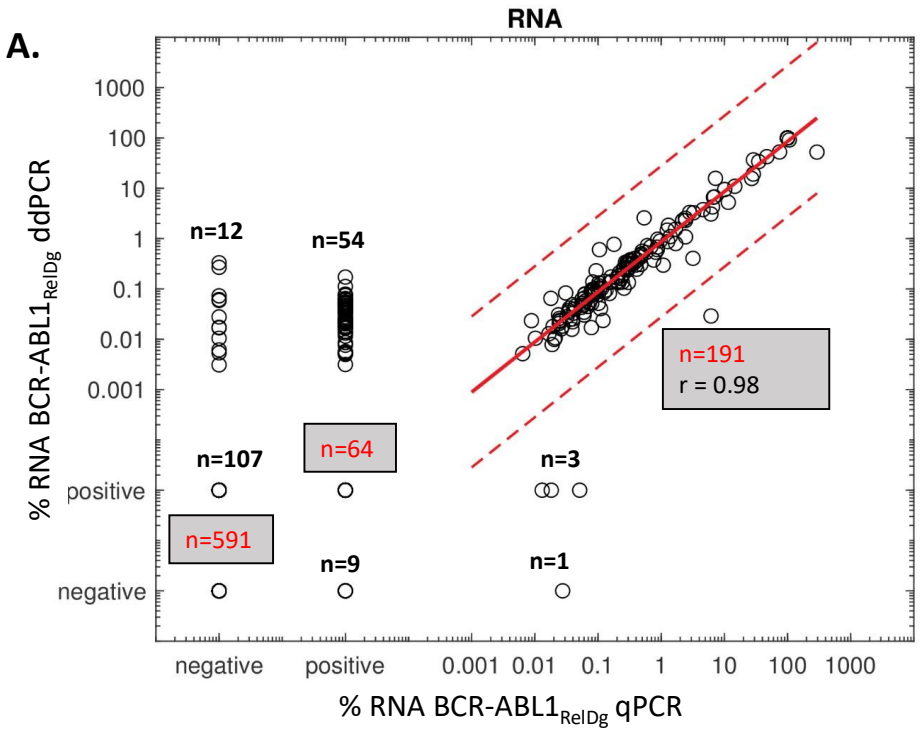

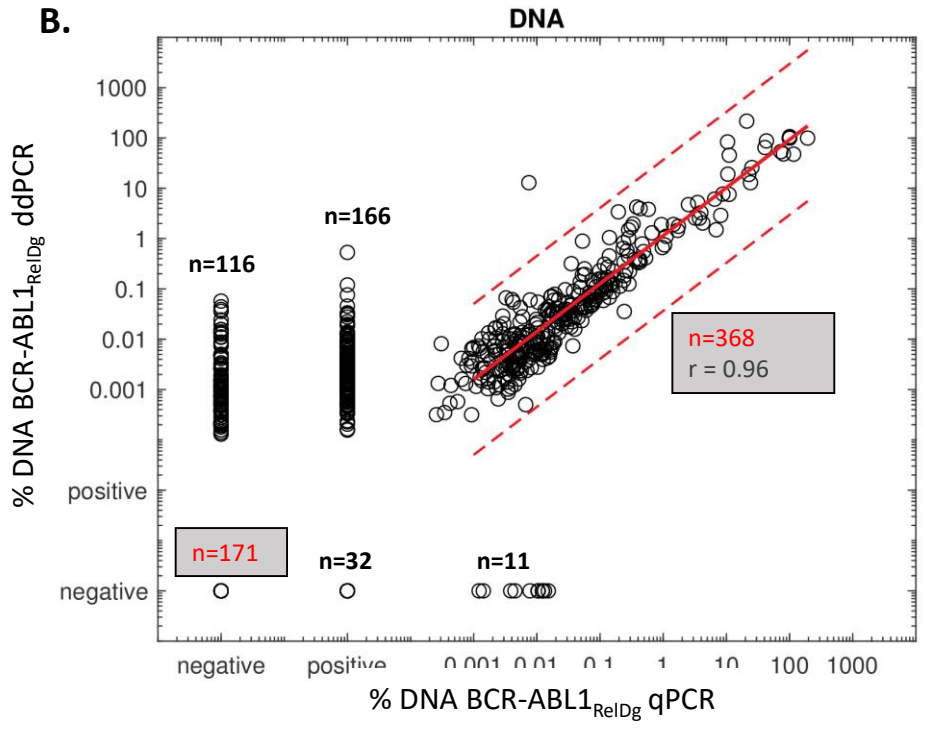

RNA	ddPCR quantifiable	ddPCR POQR	ddPCR negative
qPCR quantifable	191	3	1
qPCR POQR	54	64	9
qPCR negative	12	107	591

DNA	ddPCR quantifiable	ddPCR negative
qPCR quantifable	368	11
qPCR POQR	166	32
qPCR negative	116	171

Figure S5. Comparison of mRNA and DNA *BCR-ABL1*$_{RelDg}$ qPCR data in samples with the same level of sensitivity of measurement corresponding to MR4-MR4.5 and 10^{-4}, respectively. The same level of sensitivity of RNA and DNA measurements MR4-MR4.5 and 10^{-4} were identified in 1391 samples. The red line represents 100% concordance and dashed red lines delineate the area of 95% confidence. Of the 1383 results, 1066 (77%) results were considered concordant, i.e. *BCR-ABL1*$_{RelDg}$ at DNA and RNA level was quantifiable (n=822; r=0.92), POQR (n=20) or undetectable *BCR-ABL1* (n=224). Of the remaining 325 samples that were discordant, quantifiable *BCR-ABL1* was detected by DNA-qPCR that were POQR or negative by RNA-qPCR (n=177); samples that were POQR by DNA-*BCR-ABL1* were by RNA-BCR-ABL1 negative (n=104); *BCR-ABL1* was quantifiable by RNA-qPCR that were POQR or negative by DNA-qPCR (n=24) or *BCR-ABL1* was POQR by RNA-qPCR but undetectable by DNA-qPCR (n=12).

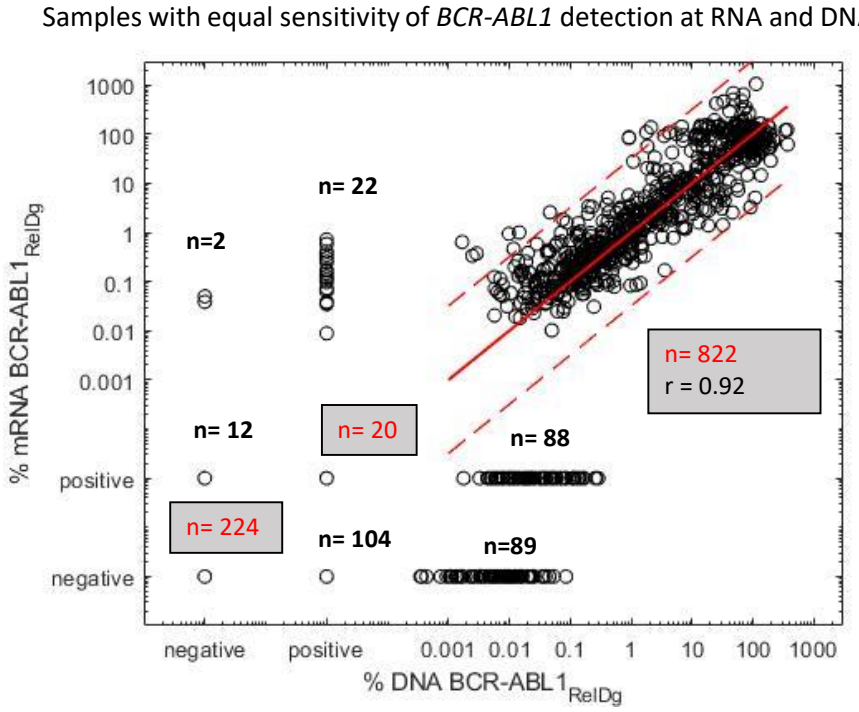

qPCR	RNA quantifiable	RNA POQR	RNA negative
DNA quantifiable	822	88	89
DNA POQR	22	20	104
DNA negative	2	12	224

Figure S6. The scheme of the mathematical model for evaluation of *BCR-ABL1* status based on DNA and RNA ddPCR data in EURO-SKI and INTReg patients with treatment stop and interuption, respectively. Ui – number of evaluated samples providing *BCR-ABL1* DNA and mRNA data before TKI stop/interruption per patient

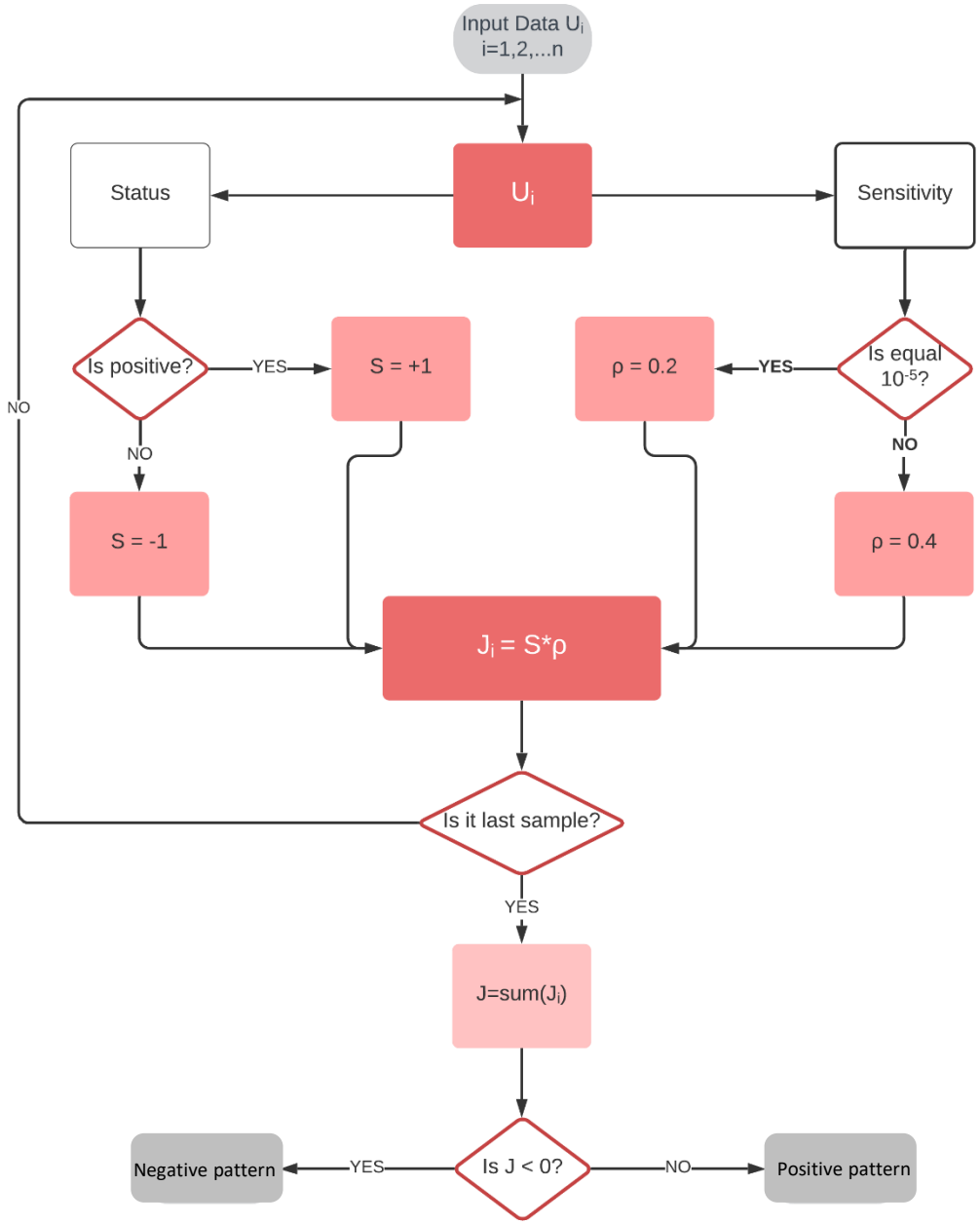

Figure S7. Probability of molecular relapse-free survival after TKI cessation/interruption in (A) patients with intermittent TKI administration or (B) EURO-SKI patients according to the traffic light stratification model. Colours of curves indicate DNA and mRNA BCR-ABL1 pattern evaluated by deterministic model (Figure S6) using data from ddPCR measurement during DMR maintenance before TKI cessation or interruption; red=double positive, yellow=DNA positive/RNA negative; green= double negative.

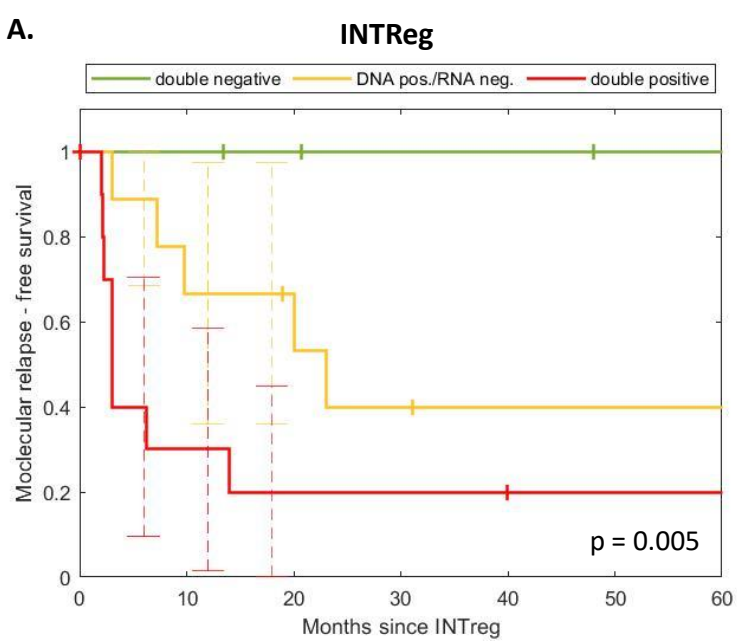

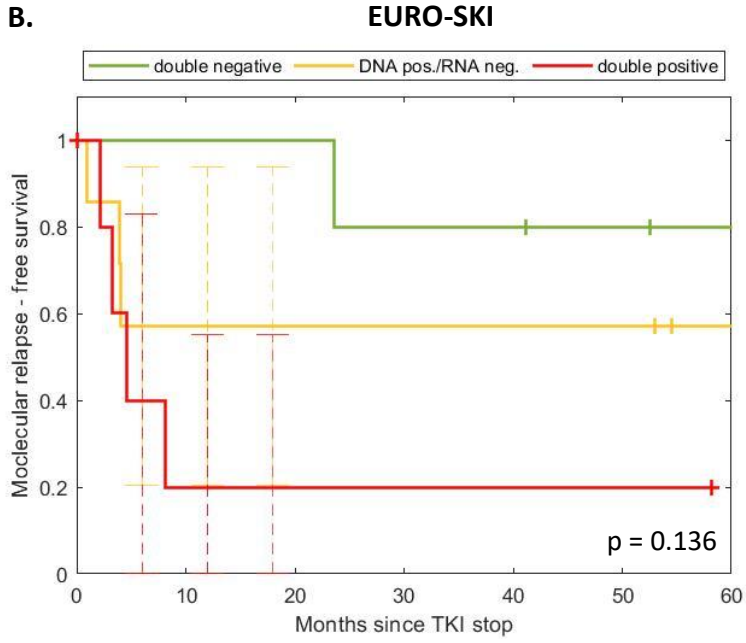

Cumulative number of molecular relapse/censored patients	Months since INTReg						
N=25	6	12	18	24	36	48	60
Double negative (n=6)	0/0	0/0	0/1	0/2	0/2	0/3	0/3
DNApos/RNAneg (n=9)	1/0	3/0	3/0	5/1	5/2	5/2	5/2
Double positive (n=10)	6/0	7/0	8/0	8/0	8/0	8/1	8/1

Cumulative number of molecular relapse/censored patients	Months since TKI stop						
N=17	6	12	18	24	36	48	60
Double negative (n=5)	0/0	0/0	0/0	1/0	1/0	1/1	1/2
DNApos/RNAneg (n=7)	0/0	3/0	3/0	3/0	3/0	3/0	3/2
Double positive (n=5)	3/0	4/0	4/0	4/0	4/0	4/0	4/1

Table S1 Characteristics of de novo diagnosed CML patients in chronic phase, one patient was diagnosed in accelerated phase

Number of patients	n=81
Median age at the time of diagnosis (years, range)	55 (19-79)
Sex	Male=43 Female=38
EUTOS score	Low=76 High=4 ND=1
Sokal score	Low=35 Intermediate=35 High=10 ND=1
Euro score	Low=36 Intermediate=41 High=3 ND=1
First line treatment (patients with reduced dose; median of reduced dose*, range)	imatinib=65 (reduced dose – 31 pts; 303mg, 205-389mg) nilotinib=14 (reduced dose – 7 pts; 518mg, 433-573mg) nilotinib + IFN=2
Median months of 1st line treatment	25.7 (0.2-45.3) months
Change therapy due to intolerance or therapy failure **Median month since 1st line treatment**	n=17 6.8 (0.2-38.5)
CML non-related death	n=4

*The reduced dose is presented as the weighted arithmetic mean of the dose in mg during the first line therapy. ND- not done

Table S2 Characteristics of 77 patients, who achieved sustained DMR during TKI treatment

	Patients with continuous TKI treatment (n=35)	**Patients in intermittent regimen (INTReg) of TKI administration every second month (n=25)**	**EURO-SKI patients (n=17)**
Median age at the time of diagnosis (years, range)	58 (29-84)	55 (31-74)	50 (32-76)
Sex	19 male; 16 female	11 male; 14 female	6 male; 11 female
First line treatment (median months, range)	imatinib=32 (84.4, 1.3-157.7) IFN=1 (11.1) nilotinib=1 (76.6) dasatinib=1 (56.9)	imatinib=23 (1 NA; 117.7 (29.8-156.6) IFN=2 (61.4; 81.3)	imatinib=14 (82.5, 10.3-142.4) IFN=2 (NA)
Duration of first line treatment stop/interruption		imatinib=21 (20.0, 3.0-76.7)	imatinib Me=6.3 (0.9-70.2)
Second line treatment (median months, range)	imatinib=1 (86.6) nilotinib=3 (36.9; 65.8; 82.2) dasatinib=6 Me=83.2 (58.8-126.1)	imatinib=2 (120.9; 187.3) dasatinib=2 (73.0; 118.1) nilotinib=1 (8.6) IFN=1 (NA)	imatinib=2 (123.3; 151.1) dasatinib=2 (19.6; 52.2)
Duration of second line treatment stop/interruption (months)		imatinib=1 (21.7) dasatinib=1 (3.0)	imatinib (41.2; 54.4) dasatinib (52.2; 71.2)
Third line treatment (median months, range)	nilotinib=1 (85.4) dasatinib=1 (39.4)	nilotinib=2 (1.7; 35.5)	
Duration of third line treatment stop/interruption (months)		n=1 (28.3)	
Fourth line treatment (months)		dasatinib=1 (117.3)	
Duration of fourth line treatment stop/interruption (months)		n=1 (59.3)	
Reasons for first line therapy switch	Therapy failure - 7 Intolerance - 3	Non-optimal response - 3 Intolerance - 2	Non-optimal response - 1 Intolerance - 3

IFN – interferon alfa; NA – not available;

Patient code	BCR-ABL1 patient-specific fusion	Breaks in introns	Note	Trancript type
AZV-E-P2	GAGCAAGACTCCGCCTAAAAAAAAAAAAAAAAAAAGTTCCTAGAAACAGCAAAATGTGGAGACAGAAAGCTTACCAGGGATTGT TGGGGAATGAAAAAAAAAAAAAATCTTAAATAGCTCTAGTTCCCTGAA	BCR: 22: 23633469; intron 14 ABL1: 9: 133707717; intron 1b		b3a2
AZV-I-P3	CACATATGCTCAGTCACACACACAGCATACGCTATGCACATGTGTCCACACACACCCCACCCACATCCCACGTCACCCCGACCCCC TCTGCTGTCCTTGGAACCATCGATTTGCTGAGCATACTTCTCAGATGTGATGGTTTCGCCG	BCR: 22: 23632288; intron 13 ABL1: 9: 133634243; intron 1b		b2a2
AZV-E-P5	CCACGTCACCCCGACCCCCTCTGCTGTCCTTGGAACCTTATTACACTTCGAGTCACTGGTTTGCCTGTATTGTGAAACCAACTGGA TCCTGAGATCCCCAAGACAGAATTAGTAGAGATGGGGTTTCTCCATATTGGTCAGGCTGGTC	BCR: 22: 23290173; intron 13 ABL1: 9: 133600945; intron 1b		b2a2
AZV-N-P6	GGATCGAGTAATTGCAGGGGTTTGGCAAGGACTTTGACAGACATCCCCAGGGGTGCCCGGGAGTGTGGGGTCCAAGCGATCCT TCTGTCGCGGCCTCCCANANCGCTGGGGATACAGGTGTGAGCCACCATGCCNGGCCTCTTTACTC	BCR: 22: 23632884; intron 14 ABL1: 9: 133601967; intron 1b		b3a2
AZV-E-P7	GTCAAGCTGTTTTGCATTCACTGTTGCACATATGCTCAGTCACACACACAGCATACGCTATGCACATGTGTCCACACACAGACTG GACTGACTGAAAGTTTATGGACCCAGAAATTTAATTCCAGCATTGAGGCTGATCTTTTGTTTGGATTG	BCR: 22: 23632239; intron 13 chr9: 133584750; between EXOSC2 and ABL1	intergenic region	b2a2
AZV-E-P9	ATCATGATGAGTATGTTTTTGGCCCATGACACTGGCTTACCTTGTGCCAGGCAGATGGCAGCACATAAAAATCTATAAAACAGAT CCTTCTAAAATTACAGAGATTCCTTGAACTGGAGGATAATAGCGAAGGANCCACAAAGGAAA	BCR: 22: 23632422; intron 13 ABL1: 27 bp inversion ABL1: 9: 133721768; intron 1a		b2a2
AZV-E-P11	GAAAGGGTCCCCACTACCAGGCCTCTCCATCCCCAGTCTCAGGTAGTTTTTCTAAAATGCAAACCCCACATCTCTTTGATTCATCTT GTCTGTTAAATTTCTTTATAAAATTTGTTTAGTTGATGACACACCTGACTCTAATATAAGAGTT	BCR: 22: 23634153; intron 14 ABL1: 9: 133623700; intron 1b		b3a2
AZV-E-P12	GACAGACATCCCCAGGGGTGCCCGGGAGTGTTGGGTCCAAGCCAGGAGGGCTGTCAGCAGTGCACCTTCACCCCACAGCAGAG CAGACTTTTGCTGGTGATAGGACAGATTATCCTGAAAATTGACCTGACAAAAATACTTAGA	BCR: 22: 23633182; intron 14 ABL1: 9: 133648269; intron 1b		b3a2
AZV-E-P13	AACAATGGCGTGTACACCTCTCTGTCCCCACCAGTGCAGGGCCCTTCTCATCGTAGGGGCTTTAGCTGGGGTTTGTGGATCGACT GAGTGAACGAATGTTGTGGGAAGTGAACATGTAGGAGCTGTTATCCCTTGCCAGTTTCATGCTTCACTGTCCATCTCCTGGCCAA ATAGAGA	BCR: 22: 23634495; intron 14 ABL1: 9: 133621353; intron 1b		b3a2
AZV-E-P16	GTGAAACCAACTGGATCCTGAGATCCCCAAGACAGAAATCATGATGAGTATGTTTTTGGCCCATGACACTGGCTTATGTGTGTGT GCTTGTGTGTGTGTGTGTTTTAATAATTTTAACTTCTCTGGGTGAAGGTGTAAATTACAAAAT	BCR: 22: 23632399; intron 13 ABL1: 9: 133721487; intron 1a		b2a2
AZV-E-P17	CCACACAGTGTCCACCGGATGGTTGATTTTGAAGCAGAGTTAGCTTGTCCAGGCTGGAGTACAGTGGCNCGATCTCNGCTCACT GCAACCTCTGCCTCCCCGGTTCNAGTGATNCNCCNGCCNCAACCTCCCGAGTAGCTGGGACT	BCR: 22: 23632470; intron 13 ABL1: 9: 133626571; intron 1b		b2a2
AZV-S-P18	TGTTGGGGATGGGGTTGGGAGAGAGGACTAACTGCAGATGAACCCAAGGGGGACTTTTTAGGTGAGAGCAGTGTCGTGAAAA GACTGTGGTGCTGTTTGCGCTCACATTTACATTTCCTAAAATTCTTGAAACAGCCTTTAAATAATGAGAACGAAGTGAAATAAAG ACATTAGATAAATAAAAACAAAAAGAATTT	BCR: 22: 23633585; intron 14 ABL1: 9: 133666684; intron 1b		b3a2
AZV-E-P19	TCACGCCAGACCACAATTAGGTGTTTAATTTTTAAAAAGAAAGTTACAACCTTTTTTTTTTATTTTTATTTTTTCTGATTCTGCAAAT AACACCTGCTCTTACAGACCACTGCTTCCTCCGTAGTTCACTCTTCACCTCCTTTGGGTCTTTGCTCAGTTGTCATCTTCAGTGATG GCTCTTCTGATCACCTTATTTAATTTTTATTTTTTAATTAAAAATTTTTTTTGTG	BCR: 22: 23634672; intron 14 ABL1: 9: 133691628; intron 1b		b3a2
AZV-E-P20	TCCGTTAAATGCCATTCTCCATCAGTGAGGCTTCTTAGTCATCTCTGGCTGCCTGGCCAGGCCCTGGCTGTGGCCTCCTCCCTGGT CTTTGTAGCTCTGGATATCCCTGCAGAAAGGGAAAATAAATTCATAGGTTTGTTTGTTCTTTTTTAGTGTCAATTTTTAAAACTATC TCTTTTTTAATTAAAAAAAATAGAGATGGGTCTCACTATGTCGCCCAGGCT	BCR: 22: 23634094; intron 14 ABL1: 9: 133716014; intron 1a		b3a2
AZV-S-P21	CTCCGTGTACAGGGCACCTGCAGGGAGGGCAGGCNGCTAGCCTGAAGGCTGATCCCCCCTTCCTGTTAGCACTTTTGATGGGAC TAGTGGACTTTGGTTCAGAAGGAATTGACAGATCTTTGAAGTATTTGAGGGAAAATGGTGATAGGTATATAGAAGACTAAATGA AAACAAGGCAATATCTCTAGGATAAACAAAGATGTATAATAAAGGAAACAT	BCR: 22: 23631930; intron 13 ABL1: 9: 133705029; intron 1b		b2a2

AZV-E-P22	CGTGGTCTGCTCTCCCTCCGTTAAATGCCATTCTCCATCAGTGAGGCTTCTTAGTCATCTGCTTTGGATTCTAGTTTTTAAGCCCTTAACAGTATCATTCAGGGCCTATGTTCTCAGGACCTCTTGAGACTGTGCCTCGGTTTTTAAAAAA	BCR: 22: 23634020; intron 14 chr9: 133583758; between EXOSC2 and ABL1	intergenic region	b3a2
AZV-S-P23	GGATCGAGTAATTGCAGGGGTTTGGCAAGGACTTTGACAGACATCCCCAGGGGTGCCCGGGAGTGTTGGGTCCAAGCCAGGAGGGCTGTCAGCAGTGCACCTTCACCCCACAGCAGAGGTATAATTTACATATCATAATATTCCCCTTCTTTATTATACAGTTCTATGGACTTTGACAAATACATACACTTGTGAAATTGCCACCCCTTTTGAGATACAG	BCR: 22: 23632972; intron 14 ABL1: 9: 133645078; intron 1b		b3a2
AZV-I-P24	GCCGGCACTTTTGGTCAAGCTGTTTTGCATTCACTGTTGCACATATGCTCAGTCACACACACAGCATACGCTATGAGGACAGCTGAGGAAGGGCTTGGCTGACAAAATGCCTTCCGACAGAGCCCTAACTACTCCACGTAAACCTAGG	BCR: 22: 23632221; intron 13 chr9: 133581642; between EXOSC2 a ABL1	intergenic region	b2a2
AZV-E-P25	CCAAACCAAACCTATTATTCATGGACCCCAAACTTGTTCCTCTTATGTCCTGTCCCTTTGAGGGGCACCACCATCCACCCGCATGGCCAAGCCAGAAACCGTGGTCTGCTCTCTCCCAAAGTGCTGGGATTACAGGCGTGAGTCACCG	BCR: 22: 23633973; intron 14 ABL1: 9: 133605684; intron 1b		b3a2
AZV-N-P26	AACCCTACACTTGGAATGGATGAATTACATGACATGCAGATTGCACCTTCATAACATAATCTTTCTCCTGGGCCCCTGTCTCTGGCTGCCTCATAAACGCTGGTGTTTGCTGAGGCGGGTGGATCACGAGATCAGGAGATCGAGACAATCCTGGCTAACACGGTGAAACCCTGTCTCTACTAAAAAAATACAAAA	BCR: 22: 23633696; intron 14 ABL1: 9: 133679507; intron 1b		b3a2
AZV-E-P27	TTTAATTTTTAAAAAGAAAGTTACAACCTTTTTTTTTTATTTTTATTTTTTCTGATTCTGCAAATAACACCTGCTCTTACAGACCATGTGGGTGATGTGGAAAAGACTGTGTATCGTATGTATGTTTATATGTATATCAGATGTACGCACATTAGTATGTGCTATTAAGATACTTTATATTATA	BCR: 22: 23634693; intron 14 ABL1: 9: 133618150; intron 1b		b3a2
AZV-N-P28	ACACTGGCTTACCTTGTGCCAGGCAGATGGCAGCCACACAGTGTCCACCGGATGGTTGATTTTGAAGCAGAGTTCAAATATTTAAAAGTGCTTAGAACAGTTACAGCACATAGTAAATGCTATATATCTGCTTGTTAAATAAATAAAAATTTAAGTTTCCAAATAATCTGTATTTCACAT	BCR: 22: 23632462; intron 13 ABL1: 9: 133646057; intron 1b		b2a2
AZV-E-P29	TCTCCTCCCAGGAGTGGACAAGGTGGGTTAGGAGCAGTTTCTCCNTGAGTGGNTGCTGCTGTACCCTATTCAGTGAGGGAGGGCACTCNCTCAGCAAATGTGCCGGGAATCAGTGG	BCR: 22: 23632016; intron 13 ABL1: 9: 133639200; intron 1b		b2a2
AZV-N-P30	CCCAGCCCACTCTTCTCCAGGCCTCGCCTCCCTCCCTTCCCCCTGCACCCCACGACTTCTCCAGCACTGAGCTGCTTCCTGTGCCCCACAGTGGCCTGGAGTCCCCTTTGCCTTAACTCTTTGCCCCATAGTACAGCGGGGTCTGCTCTGATTGTATGTTTTTAGCTTGGAGGAGAGAAGCCTAAGGGAAGATGTGTTTGCTGTTTTGAAAATATTTATTGTCGCTGGGCGCGGTGGCTCACGCCTGTAATC	BCR: 22: 23634332; intron 14 ABL1: 9: 133629244; intron 1b		b3a2
AZV-I-P32	GGCTTACCTTGTGCCAGGCAGATGGCAGCCACACAGTGTCCACCGGATGGTTGATTTTGAAGCAGAGTTAGCTTGTCACCTTTAACCAAGCAGGCCAGGCACGGTGGCTCACGCCTATATCCCAGCACTTAGGGAGGCCAAGGCGGGCAGATCACCTGAGGTCAATAGTTCGAG	BCR: 22: 23632474; intron 13 EXOSC2: 9: 133579624: ; exon 9	alternative splicing	b2a2
AZV-N-P33	AGGGAAGAGAATCGCTTGAACCCAGGAGGCGGAGGTTGCAGTGAGCCGAAGCTCCAGAAATGTGGGATACTCAGCACTGGAGACATTTG	BCR: 22: 23633345; intron 14 ABL1: 9: 133656069; intron 1b		b3a2
AZV-E-P34	GCTGTCCTTGGAACCTTATTACACTTCGAGTCACTGGTTTGCCTGTATTGTGAAACCAACTGGATCCTGAGATCCCCAAGACAGAAATCATGATGAGTATGTTTTTGGCCCATTACTTCATCTATAGCTTTGCTGAGGTTTTTTTTTTTT	BCR: 22: 23632387; intron 13 ABL1: 9: 133602597; intron 1b		b2a2
AZV-I-P35	GTGCACCTTCACCCCACAGCAGAGCAGATTTGGCTGCTCTGTCGAGCTGGATGGATACTACCCGCTTAACTTCCCAATTTGCTTCAAATGCCAAATGATCATAGAATGGTCAACATTGAGTTTTTCAGCAACTTCTTTTATGGTTGTAAGAGGATCAGCTTCT	BCR: 22: 23633009; intron 14 ABL1: 9: 133634548; intron 1b		b3a2
AZV-N-P36	GGTGGATCGCTTGAGCTCAGGAGTTGGAGACCAGCCTGACCAACATGGTGAAACCCTGTGTCTACTAAAGCTACAGAACAAACATGTATTTTCAGAAGCTTGCTTGCACCTCTGCCACTCTGTCCTTTTCNNNCTCCTACTCN	BCR: 22: 23633235; intron 14 ABL1: 9: 133610761; intron 1b		b3a2
AZV-I-P37	TCGTGAAAAGACTGTGGTGCTGTTTGCGCTCACATTTACATTTCCTAAAATTCTTTAAACCCTACACTTGGAAAGTTTGCAAATTTGTTAGGCCACATTCAAAGCCGTCCTGGGCCATA	BCR: 22: 23633604; intron 14 ABL1: 9: 133716816; intron 1a		b3a2
AZV-N-P38	ATGACACTGGCTTACCTTGTGCCAGGCAGATGGCAGCCACACAGTGTCCACCGGATGGTTGATTTTGAAAGTTGTATTACTAGTTTTGGGGAGTTTGCAGACAATTGAATATTCTATAGGCTGTGTTGCAGCTTTAGATGGATCGACCTGTCATGTTTTTGAGGTTATCC	BCR: 22: 23632453; intron 13 chr9:133582448; between EXOSC2 a ABL1	intergenic region	b2a2

	AGGCTGTAT			
AZV-N-P39	TCCTGGGAGCTGGTGAGCTGCCCCCTGCAGGTGGATCGAGTAATTGCAGGGGTTTGGCAAGGACTTTGACAGACATCCCCAGGGGTGCCCGGCATTGTTCTATCAAAGAAGCTTCCACCATAAATGTGGTTTGATGGTGCATGCTACCTGCTACTCAGCCTAGCTGTCAAAGCAAC	BCR: 22: 23632914; intron 14 ABL1: 9: 133713316; intron 1a		b3a2, b2a2
AZV-E-P40	TGGGCCCCCCCGTTTCCGTGTACAGGGCACCTGCAGGGAGGGCAGGCAGCTAGCCTGAAGGCTGATCCCCCCTTCCTGTTAGAGGAGACTCCGTCTCAAAAAAAAAAAAAAAAAAAAAAAAAATTTACTATCATGTAAAGGGGAGTTGGTCTCACCCTACACTGCTTTGGAAGGCAC	BCR: 22: 23631889; intron 13 ABL1: 9: 133629877; intron 1b		b2a2
AZV-I-P41	GATCGCTTGAGCTCAGGAGTTGGAGACCAGCCTGACCAACATGGTGAAACCCTGTGTCTACTAAAAATACAAAGATTAGCCGGGCTAGGCAGTGGGCACCTGTAATCACAACTGCTTGGGAGGCTTTTTTAATTAAAAAAAATAGAGATGGGTCTCACTATGTCGCCCAGGCTGGT	BCR: 22: 23633293; intron 14 ABL1: 9: 133716070; intron 1a		b3a2
AZV-E-P42	TGGGGATGGGGTTGGGAGAGAGGACTAACTGCAGATGAACCCAAGGGGATCCCACGTTGTGGAATTTCCACCGTTAATTGGGACTGTGTGTTAAAAAGATCGACCCGTGTTTGTGAA	BCR: 22: 23633506; intron 14 ABL1: 9: 133711328; intron 1a		b3a2
AZV-E-P43	CTCGAGGCCGGGCGCAGTGGCTCATGCCTGTAATCCCAGCACTTTGGGAGGCTGAGGCAGGTGTTCCTCCTTTTGTGTCTCTGAGTAGTATTCTCTTGCATAGATGTACCACAGTTTGTTTATCCATTCACCAGCTGAAGGACAGTGCTCCAGGGTCCTAGAGCACAGAACTCTGG	BCR: 22: 23633170; intron 14 ABL1: 9: 133645407; intron 1b		b3a2
AZV-E-P44	GTTGCAGTGAGCCGAGCTTGTGCCACTGCATTCCAGCCTGGGCGACAGAGCAAGACTCCGCCTCAAAAAAAAAAAAAAAAAAGTTCCACCGCTGTCTGCTAAACTGCATAGAATCTGGAAGCCATGGACCCACAGGATGCCTCCCACCTTCTTCTGCCTACCTCTGTGTTCTGTCACC	BCR: 22: 23633414; intron 14 ABL1: 9: 133604670; intron 1b		b3a2
AZV-E-P45	GGAAGAGCTATGCTTGTTAGGGCCTCTTGTCTCCTCCCAGGAGTGGACAAGGTGGGTTAGGAGCAGTTTCTCCCTGAGTGGCTGCAGTGTAGTTCCCTGTGTGTCCCTGATATCTCTTCAGGGGTTGAGAGGCTAAAACTATTTTCTTGTTAATAGAGTACCAAGGTCTTGTCTCTT	BCR: 22: 23632008; intron 13 ABL1: 9: 133591176; intron 1b		b2a2
AZV-N-P46	GGCTGCCTGGCCAGGCCCTGGCTGTGGCCTCCTCCCTGGTCTTTGTAGCTCTGGATATCCCTGCAGAAAGGGTCCCCACTAAATCTGAGAGGTGGAGGTTGCAGTGGGCCGAGATCAATCACACCACTGCACGCTAGCCTGATGAAGGAAGGAGAAACAGTGATTCATTTGTTTT	BCR: 22: 23634101; intron 14 ABL1: 9: 133671816; intron 1b		b3a2
AZV-N-P47	TCCAGACTGTCCACAGCATTCCGCTGACCATCAACAAGGAAGGTGGGCCCCCCCCGTCTCCGTGTACACAGTAGCTTGAAGGTTTAAGTGATAACTTTATTTTGCAAAACTGACCACATTCTTTTGTTGCTTAGGTGTCTCCCCTTTAAGGGATTCTGATGTCTAGCAGTCTCAATGG	BCR: 22: 23631833; intron 13 ABL1: 9: 133670906; intron 1b		b2a2
AZV-N-P48	TGGGGATGGGGTTGGGAGAGAGGACTAACTGCAGATGAACCCAAGGGGGACTTTTTAGGTGAGAGCAGTGTCGTGAAAAGACTGTGGTGCTGTTTGCGCTCACATTTACATTTCCTAAAATTCTTTAAACCCTACACTTGGTTATATTATATAATATATACTGTATAATACCGTATATTATAAAGCATTCATAAAATGAAAATGAAGATGAAATAAATTGCATTGTAAATATTTAAAACT	BCR: 22: 23291415; intron 14 ABL1: 9: 130742830; intron 1b		b3a2
AZV-N-P49	CCCTCGTGGGCCTCCCTGCATCCCTGCATCTCCTCCCGGGTCCTGTCTGTGAGCAATACAGCGTGACACCCTACGCTGCCCCGTGGTCCCGGGCTTGTCTCTCCTTGCCTCAAGATCTCACTCTGTCACTCAGGCTGGAGTGCAGTGGCAATCATAGCTCACTGCAACCTCCGTC	BCR: 22: 23633806; intron 14 ABL1: 9: 133603475; intron 1b		b3a2
AZV-N-P50	GAATGTTGTGGGAAGTCCCGTTTCCCAGCCGCACCCAGGGAAATTCCACAGAGCGGGCAGGGGCATCGCATTTCATTTCAGGTTCTAGTTCAAATTGAATCCAAGTGAAGTGACCCCATAATACATGTTAATTGTGGAAAAAAATTTAAATTTAGTAAAGTAAAGAATAGAGCATGTCA	BCR: 22: 23292363; intron 14 ABL1: 9: 130763188; intron 1		b3a2
AZV-S-P51	GCCAGGAGGGCTGTCAGCAGTGCACCTTCACCCCACAGCAGAGCAGATTTGGCTGCTCTGTCGAGCTGGATGGATACTACTTTTTTTTTCGTGATTACATTTATGCCCACTAGGATGACGGAGGATAATGCCCCCATCTCAANATTGTTAATCACATCTCCAAANACCCTTTTCTCCC	BCR: 22: 23633019; intron 14 ABL1: 9: 133623126; intron 1b		b3a2
AZV-E-P52	CTAAAATTCTTTAAACCCTACACTTGGAATGGATGAATTACATGACATGCAGATTTTTAGTGTCAATTTTTAAAACTATCTCTTTTTTAATTAAAAAAAATAGAGATGGGTCTCACTATGTCGCCCAGGCTGGTCTCAAACTCCTGGGCTCAAGCAATCCTCCCACCTCAGCCTCCCAAA	BCR: 22: 23633628; intron 14 ABL1: 9: 133716042; intron 1a		b3a2
AZV-E-P53	TGAACCCAAGGGGGACTTTTTAGGTGAGAGCAGTGTCGTGAAAAGACTGTGGTGCTGTTTGCGCTCACATTTGGGTTACTGTTTGTACTGTTGCAGCCTGACATTTTTTGGATTGTGTC	BCR: 22: 23633568; intron 14 ABL1: 9: 133590657; intron 1b		b3a2
	AGGAGTTGGAGACCAGCCTGACCAACATGGTGAAACCCTGTGTCTACATTATGAGTCAGATTTTCCTGCATTTTTGCATGTTAAA	BCR: 22: 23633228; intron 14		b3a2

AZV-N-P55	AGGAGTTGGAGACCAGCCTGACCAACATGGTGAAACCCTGTCTCTACTAAAAATACAAAAATTAGCCAGGCATGGTGGCACATGCCTGTAATCCCAGCTACTCAGGAGGCTGAGGCAGGAGAATCGCTTGAACCCAGGAGGCAGAGGTTGCAGTGAGCCGAGATCGCGCCACTGCACTCCAGCCTGGGCGACAGAGCGAGACTCCGTCTCAAAAAAAAAAAAA TAATTTTGATTGTATGCCAGACATGTGGGTGTTAT	ABL1: 9: 133604246; intron 1b		
AZV-N-P56	CCTCTCCCCTAGCCTGTCTCAGATCCTGGGAGCTGGTGAGCTGCCCCCTGCAGGTGGATCGAGTAATTGCAGGGGTTTGGCAAG GACTTTGACAGACATCCCCAGGGGTGCCCGGGAGTGTGGGGTCCAAGCCAGGAGGGCGGGTGAAGGTGTAAATTACAAAATA AAGGACCATGTAGAAATAGATAAAATGACTTTCATCAAGCTCAAAATGTGGGAAATAATACTTTTCCTCTAAGCTCATATTTTGA	BCR: 22: 23632940; intron 14 ABL1: 9: 133721535; intron 1a		b3a2
AZV-I-P57	GAGCTGGATGGATACTACTTTTTTTTTCCTTTCCCTCTAAGTGGGGGTCTCCCCCAGCTACTGGAGCTGTCAGAACAGTGAAGGC TGGTAACACATGAGTTGCTCCTCAGGGTCAGACACCTCCTGTCCCTTACTCTGTAAGGCACAGCTTCTACCTCAGGATCCAAAAT GCCCACGCCAGCTGCCATGGCCCCTCACAGGCAGTGGACACCAGAAAGAGGAGAGGGAGTGCGT	BCR: 22: 23633092; intron 14 ABL1: 9: 133698911; intron 1b		b3a2
AZV-S-P58	GCCTCTCCATCCCCAGTCTCAGGTAGTTTTTCTAAAATGCAAACCCCACCCTGCAACTTATCTATAGTCCCAGCTACTTGAGGGGC TGAGGCTGAAGTATCTCTTGAACCCAGGAGGTT	BCR: 22: 23634166; intron 14 ABL1: 9: 133650106; intron 1b		b3a2, b2a2
AZV-N-P59	GCTGTGGCATCACTGTGTAACAATGGCGTGTACACCTCCTGAGCAAGAGTAAGACCCTGTCTCAAAAAACCAAAACAAAATCAA GTCTCCCTCAGTCTTCCT	BCR: 22: 23634406; intron 14 ABL1: 9: 133622736; intron 1b		b3a2
AZV-E-P60	CCGCTGTGGAGTGTTTGTGCTGGTTGATGCCTTCTGGGTGTGGAATTGTTTTTTCCCGGAGTGGCCTCTGCCCTCTCCCCTAGCAT TTTTTAGTCAGGTTTATTGAGGTATAATTTACATATCATAATATTCCCCTTCTTTATTATACAGTTCTATGGACTTTGACAAATACAT ACACTTG	BCR: 22: 23632812; intron 14 ABL1: 9: 133645055; intron 1b		b3a2
AZV-E-P61	TCGGGCAGGGTGTGGGGAAACAGGGAGGTTGTTCAGATGACCACGGGACACCTTTGACCCTGGCCGCTGTGGAGTGTTTGTGC TGGTTTCCCCCAATGTTTTGTTTTTGTTGCTATTGTTTTGAAATAGGGTCTTGCTCTATCGTCCAGGCTGGAGTGTAGTGGTGCAA TCATGGCTCACTGAA	BCR: 22: 23632752; intron 14 ABL1: 9: 133648828; intron 1b		b3a2
AZV-I-P62	GCCAAGCCAGAAACCGTGGTCTGCTCTCCCTCCGTTAAATGCCATTCTCCATCAGTGAGGCTTCTTAGTCATCTCTGGCTGCCTGG CCAGGCCCTGGCTGTGGCCTCCTCCCTGGTCTTAGGTAAATCAGATATTAAATTCTTTATAGACTTCTGGTTCATATTCCAGTTGC CCTCAATTTATACACCTACTACTAGCATTGTATGAGAGTGCCCGTTTCTCTGAAATCTTACCCACA	BCR: 22: 23634065; intron 14 ABL1: 9: 133724686; intron 1a		b3a2
AZV-N-P63	GGACTAGTGGACTTTGGTTCAGAAGGAAGAGCTATGCTTGTTAGGGCCTCTTGTCTCCTCCCAGGAGTGGACAAGGTGGGTTAG GAGCAGATGTACGCACATTAGTATGTGCTATTAAGATACTTTATATTATATAATATATACTGTATAACACCGTATATTATAAAGCA TTCATAAAATGAAAATGAAGATGAAATAAATTGCATTGTAAATATTTAAAACTTTAAAAAATGCGTTACTGGTACAAAATTTTTTT	BCR: 22: 23631989; intron 13 ABL1: 9: 133618180; intron 1b		b2a2
AZV-S-P64	GCCTGTATTGTGAACCAACTGGATCCTGAGATCCCCAAGACAGAAATCATGATGAGTATGTTTTTGGCCCATGACACTGGCTTAC CTTGTGCCAGGCAGATGGCAGCCACACAGCGGAAGGTGAAGGTTGCAGTGAGCAGAGATCACGCCATTGCACTCCAGCCTGAG TGTCAAGAACGAGACTCCGTCTCGAGAAAAAAAAAAAA	BCR: 22: 23632429; intron 13 ABL1: 9: 133724250; intron 1a		b2a2
AZV-E-P65	GAGACCAGCCTGACCAACATGGTGAAACCCTGTGTCTACTAAAAATACAAAGATTAGCCAGGCTAGGCAGTGGGCACCTGTAAT CACAACTGCTTGGGGTCACCTTGTCCTGGGGTCCCAAGCCAGGCCTCCTGTCAGGTTCATCTGTCTCTGTTCCACCTGCACTCACA CCCAGT	BCR: 22: 23633287; intron 14 ABL1: 9: 133706608; intron 1b		b3a2
AZV-N-P66	CACAGTGTCCACCGGATGGTTGATTTTGAAGCANAGTTAGCTTGTCACCTGCCTCCCTTTCCCGGGACAACAGAAGCTGACCTCT TTGATCTCTTCCTACCTTCCTACCTCCTGGCTGTGTGAACTTGGACAGAATACTTCCCCCTCTCCCTCCAGTCAGTTTTCTTACTTGT GAAAT	BCR: 22: 23632517; intron 13 ABL1: 9: 133707881; intron 1b		b2a2
AZV-E-P67	GAGTATGTTTTTGGCCCATGACACTGGCTTACCTTGTGCCAGGCAGATGGCAGCCACACAGTGTCCACCGGATGGTTGATTTTGA AGCAGAGTTAGCTTGTCACCTGCCTCCCTTTCCCGGGACGTGAGCAGGGGAATCGAGGAACCTCTCAGGGCTTTGTGTTGGGAC ACTGACTCACTGCATTAGTACTTTCTAGACTGTGAGCAGGGGAATTGAGGAACCTCTCAGGGCTTT	BCR: 22: 23632492; intron 13 ABL1: 9: 133653642; intron 1b		b2a2
AZV-N-P68	CACATGAGGTGCTGGTGTTCACGCCAGACCACAATTAGGTGTTTCTTAGGATGTATTCTGATCTTTTTCAAGTGGCTACATCACTG ACCCTCATAAAATAACGGAAAATATTGGGAGAT	BCR: 22: 23634590; intron 14 ABL1: 9: 133635866; intron 1b		b3a2
AZV-N-P69	GCCTGTAATCCCAGCACTTTGGGAGGCTGAGGCAGGTGGATCGCTTGAGCTCAGGAGTGGACTGGGATAGAAAGTATTTGTCTT TCATTTTAAGCCCTTCTGTACGATTTGAC	BCR: 22: 23633190; intron 14 ABL1: 9: 133728493; intron 1a		b3a2
AZV-E-P70	CCGGGAGTGTGGGGTCCAAGCCAGGAGGGCTGTCAGCAGTGCACCTTCACCCCACAGCAGAGCAGAACAGCACAAGGCAAGC AAATATCTGGGCCTATATTAACAGACGGTATTCAAGGATATGGCTAGAATTTCCAAAATGCCTAATAATGTGTAATTCTTGGCAT TAAGCCGCC	BCR: 22: 23632973; intron 14 ABL1: 9: 133708512; intron 1b		b3a2

AZV-N-P71	TGTTTTTTCCCGGAGTGGCCTCTGCCCTCTCCCCTAGCCTGTCTCAGATCCTGGGAGCTGGTGTAAAAACAATAACAATCAGAAT AAGAATAAAAATGAATTATTTTTCTTTTATTTATTTATTTATTTATTTTTGATACATGGTCTCTGTCACCCAGGCTGGAGTGCAGTG GCAAGATCACAGCTCACTGCAGCCCCAACCTGCCTCAGCCCCCCAAGCAACTGGGACTACAGGCACG	BCR: 22: 23632837; intron 14 ABL1: 9: 133703422; intron 1b		b3a2, b2a2
AZV-E-P72	ACTCAACCTTGCATCCCCAAACCAAACCTATTATTCATGGACCCCAAACTTGTTCCTCTTATGTCCTGTCCCTTTGAGGGGCACCAC CATCCACCCGCATGGCCAAGCCAGAAACCGTGGTTAACCTAAAAAGCTGTGGTGAGGCTGGGCGCGGTGGCTCATGCCTGTAAT CCCAGCACTTTGGGAGGCCGAGGCAGGCAGATCACCTGACGTCAGGCGT	BCR: 22: 23633964; intron 14 ABL1: 9: 133651678; intron 1b		b3a2
AZV-N-P73	TTCACGCCAGACCACAATTAGGTGTTTAATTTTTAAAAAGAAAGTTACAACCTGAGGTCTGTTAGATCAGGAATTCAGAAGTGGG TTAGCTGAGTGGTTCTAGCT	BCR: 22: 23634615; intron 14 ABL1: 9: 133638838; intron 1b		b3a2
AZV-N-P75	GCTGTTTGCGCTCACATTTACATTTCCTAAAATTCTTTAAACCCTACACTTGGAATGGATGAATTACATGACATTGATGTCTATAAC CAGTTAATTAGGGTTACTGTTTGTACTGTTGCAGCCTGAC	BCR: 22: 23633623; intron 14 ABL1: 9: 133590934; intron 1b		b3a2
AZV-E-P76	GCACGGCTTCTGTTCCTAGTCACAAGGCTGCAGCAGACGCTCCTCAGATGCTCTGTGCCTTGGATCTCTCTCATCTCTTCTTTTTTT TTCTTTTCTTTTTTTTTTTTTTTTTTTTTTTGAGATGGAGTCTCACTCTGTTGCTCAGGCTGGAGTGCAGTGGTGCAATCTTGGCTCACT GCAA	BCR: 22: 23632095; intron 13 ABL1: 9: 133628779; intron 1b		b2a2
AZV-E-P77	AACCCCACCCTGCAACTTACCGCCCACAGCCCAGCCCACTCTTCTCCAGGCCTCGCCTCATAGACTAAGGAGCCACATCCCTGCTC CTGGGATATCCTTTAGTCAAAGGGCTAGAAGGGTCCTGGAGGTTTGCCACTTCTCCGTGTTGAGGTACAGAGTTCCTAGACTAA GGGACT	BCR: 22: 23634206; intron 14 ABL1: 9: 133616461; intron 1b		b3a2
AZV-N-P78	GTGGCATCACTGTGTAACAATGGCGTGTACACCTCTCTGTCCCCACCAGTGCAGGGCCCTTCTCATCGTAGGGGCTTTACTGTGT TTTCTTTTGCTTGTTATGCGTAAGGTCAGATATGTTGTGTTTTGGGTCCCTGACACCTTGGGCTTGGATGAATAATGTCACTTAAG AGGAGG	BCR: 22: 23634449; intron 14 ABL1: 9: 133639955; intron 1b		b3a2
AZV-S-P79	CGCACCCAGGGAAATTCCACAGAGCGGGCAGGGGCATCGCATGAGGTGCTGGTGTTCACTCAGTTCAGGACAGAACCGTGCTT GTGCTTCAGATC	BCR: 22: 23634567; intron 14 ABL1: 9: 133598296; intron 1b		b3a2
AZV-N-P80	GATGAGTCTCCGGGGCTCTATGGGTTTCTGAATGTCATCGTCCACTCAGCCACTGGATTTAAGCAGAGAGCTTCCCACTGCTAAT GTGTCATTTTTCCTTTCTCTTGCCACTGAGTTGTTTGCTCAACTAG	BCR: 22: 23632595; exon 14 ABL1: 9: 133667633; intron 1b	non-complete exon 14	b2a2
AZV-N-P81	AAAAAAAAAAAAAAGTTCCTAGAAACAGCAAAATGTGGAGACAGAAAGCTTACCAGGGATTGTTGGGGCAGTGAGCAAGGAT TGCACCACCGCATTCCAGCCTGGGTGACAGAGTGAGACTCTGTCTCAAAAATAATAAATAAATAAATAAATAAATAAATAAATA AATAAATAAAGCT	BCR: 22: 23633464; intron 14 ABL1: 9: 133703220; intron 1b		b3a2
AZV-E-P82	TACATTTCCTAAAATTCTTTAAACCCTACACTTGGAATGGATGAATTACATGACATGCAGATTGCACCTTGTTGAGAAAGGTCTGT CGATAGTGGTTATCTTTTGAGAGTGGAATGGATC	BCR: 22: 23633636; intron 14 ABL1: 9: 133644370; intron 1b		b3a2
AZV-N-P82	TCAGTCACACACACAGCATACGCTATGCACATGTGTCCACACACACCCCACGCTTTTCCCATTTAGCCTTTTGAAACAGGATACAC AGTAGGGTGATTGGTTTGGGAG	BCR: 22: 23632245; intron 13 ABL1: 9: 133656644; intron 1b		b2a2
AZV-S-P83	TTTTATTTTTATTTTTTCTGATTCTGCAAATAACACCTGCTCTTACAGACCATGTGGGTGAAATTAGGAAGTGGGGCAAAAGCCCC AGTGCCTTCCCTTCAACCTGACGACCAGTCTACC	BCR: 22: 23634681; intron 14 ABL1: 9: 133660338; intron 1b		b3a2
AZV-N-P85	GGGTTGGGAGAGAGGACTAACTGCAGATGAACCCAAGGGGGACTTTTTAGGTGAGAGCAGTGTCGTGAAAAGACTGTGATGC TAACATGGTAATTTTTAAATTTGTGTGGTGTGCATGTGT	BCR: 22: 23633552; intron 14 ABL1: 9: 133637750; intron 1b		b3a2
AZV-N-P87	AGCAGAGTTAGCTTGTCACCTGCCTCCCTTTCCCGGGACAACAGCCCTGGCAGTCACCTGTGAGGCTTCACCCCGTCTCCCCACC CACTATAACCTCTGACTTACCTCCTTTTACACTCCTTCTTGCTGACTCT	BCR: 22: 23632495; intron 13 ABL1: 9: 133691440; intron 1b		b2a2
AZV-N-P88	CTGCTGGGTGGTTGAGGAGATGCACGGCTTCTGTTCCTAGTCACAAGGCTGCAGCAGACGCTCCTCAGACAGTCAAATTGTTTT GCCTGTTGAAGAAGGTGATCAGACCCTAATGAAACTGAAAATGAGGAGAGTGTTCCCATCTCCTGCCTGGTTCTAGCGACTCTG	BCR: 22: 23632076; intron 13 ABL1: 9: 133656246; intron 1b		b2a2

	CAAATGGGTGCCTGATTGGTCTGTTGGCTCTGAAGCCAGCCTTTGCTGGATATATTCAGCCTGTTTTG			
AZV-E-P89	CACGGCTTCTGTTCCTAGTCACAAGGCTGCAGCAGACGCTCCTCAGATGTTTTAATGAAGATATATGAACTTGAAGGGATTTATTCAATATATGACAATATTACTCAATATTACTTTTTTTTTTTTTTTTTTTGAGACAAAGTCTCGCCC	BCR: 22: 23632081; intron 13 chr9: 133583041; between EXOSC2 a ABL1	intergenic region	b2a2
AZV-E-P90	TTTGGTCTCTTGCGCAGATGATGAGTCTCCGGGGCTCTATGGGTTTCTGAATGTCATCGTCCACTCAGCCAGTAGCTGTTCCCAATGAACAAATATTTAAGTTACTTCCAATTGTCTCTAGTTAGGTTTCTCATAGGGGTTTTAATTTAATTCTCACAAAGACCCTATAGAGTGGGCCTA	BCR: 22: 23632579; exon 14 ABL1: 9: inversion	non-complete exon 14	b2a2
AZV-E-P91	GTTCCTAGAAACAGCAAAATGTGGAGACAGAAAGCTTACCAGGGATTGTTGGGGAATGGGGTTGGGAGAGAGGACTAACTGCAGATGAACCCAAGGGGGACTTTTTAGGTGAGAGCAGTGTCGTGAAAGGCTCAGGCAGTCCTCCCACCTCAGCCTCTCGAGTAGCTGGGACCACAGGTGTGCACTACCACACCTGGCTAATTTAAAAAAAAAATTTATAGAGACAGAGTCTTG	BCR: 22: 23633539; intron 14 ABL1: 9: 133601330; intron 1b		b3a2
AZV-S-P92	CACAAGGCTGCAGCAGACGCTCCTCAGATGCTCTGTGCCTTGGATCTGGCCCCACTCCCGGCAGTTGAACTAATTTGTCCCACTGTCTTGCTTCTTTGTATGGTGGGTAGTTCTGGAT	BCR: 22: 236332110; intron 13 ABL1: 9: 133678100; intron 1b		b2a2
AZV-S-P93	ACTACTTTTTTTTTCCTTTCCCTCTAAGTGGGGGTCTCCCCCAGCTACTGGAGCTGTCAGAACAGTGTTTAGGTAATTTAATTTTTTTTTTTTTTTTTTTTTTTTTTTTGGAGACGGGGTCCCACTACGTTGTCCAGGCTGGCCTCTAACTCCTGGGCTTAGGCAATCCTCCCACTTCAGCCT	BCR: 22: 23633071; intron 14 ABL1: 9: 133635337; intron 1b		b3a2
AZV-E-P94	CACATATGCTCAGTCACACACACAGCATACGCTATGCACATGTGTCCACACACACCCCACCCACATCCCATGTGTATCCTCAGTCTGATGGCGGTGGAAGTGAGGCAGCACCAAGGA	BCR: 22: 23632255; intron 13 ABL1: 9: 133643802; intron 1b		b2a2
AZV-I-P95	ACTAATCGGGCAGGGTGTGGGGAAACAGGGAGGTTGTTCAGATGACCACGGGACACCTTTGACCCTGGCCGCTGTGGAGTGTTTGTGACTTGAGGCTATTATAGTACAGCTGCTATGAACATTTGTGTATTCACCATTGTGTGAGCATATGATTTTCCCTACCTTCTTTTCTATTTCA	BCR: 22: 23633323; intron 14 ABL1: 9: 133664585; intron 1b		b3a2
AZV-N-P96	ACTAAAAATACAAAGATTAGCCGGGCTAGGCAGTGGGCACCTGTAATCACAACTGCTTGGGAGGCTGAGGGAAGAGAATCGCTTGAACCCAGGACAGAGAGAAAATGTACGGGGGAGAAGCACATTACACAGTATCAATCAGAAAGGAATATTTCTGTCTGAGCTTTCACTTTGAGTGGAGGGCAAAGAAAAAA	BCR: 22: 23633323; intron 14 ABL1: 9: 133664585; intron 1b		b3a2
AZV-N-P97	TGTTTTTGGCCCATGACACTGGCTTACCTTGTGCCAGGCAGATGGCAGCCACACAGTGTCCACCGGATGGTTGATTTTGAAGCANAGTTAGCTTGTCACCTGCCATAGTAAATGCTATATATCTGCTTGTTAAATAAATAAAAATTTAAGTTTCCAAATAATCTGTATTTCACATAAAAGAGAAGAGATGTGGGACA	BCR: 22: 23632476; intron 13 ABL1: 9: 133646091; intron 1b		b2a2
AZV-N-P98	TCGCTTGAACCCAGGAGGCGGAGGTTGCAGTGAGCCGAGCTTGTGCCACTGCATTCCAGCCTGGGCGACAGAGCAAGACTCCGCCTCAAAGAGGATTTTGACTGAGATGGGGGCAAACATGATAGACAAACTTTAGGGACAATTTAGCATTGTCTTCAAACACAGGTATGAGGGAG	BCR: 22: 23633397; intron 14 ABL1: 9: 133648185; intron 1b		b3a2
AZV-N-P99	AGTGGACAAGGTGGGTTAGGAGCAGTTTCTCCCTGAGTGGCTGCTGCTGGGTGGTTGAGGAGATCACAGGACGCGCGTTGAGTAGAAATGAGACCAGTTAGTATTGGT	BCR: 22: 23632029; intron 13 ABL1: 9: 133710180; intron 1b		b2a2
AZV-E-P100	TAGGTGAGAGCAGTGTCGTGAAAAGACTGTGGTGCTGTTTGCGCTCACATTTACATTTCCTAAAATTCTTTAAACCCTACACTTGGAATGGATGAATTAAGGTTACTGTAGTTACTTAAATTACTGTAAGTGACTGGTCGTTAAGTTAGTTTGACCCTGCCAGGTTTGGTTTTATGCTTT	BCR: 22: 23633615; intron 14 ABL1: 9: 133604389; intron 1b		b3a2
AZV-N-P101	CTCCTCTCCTCCAGCTACCTGCCAGCCGGCACTTTTGGTCAAGCTGGTTTGTCCATTTTTCTATTTATGTTTATTCCTCATTGATTTTTAGGAGTTATTTATATTTTTTTTCCTTTTTTTTTCTTTGTTTGAGGCAGAGTCT	BCR: 22: 23632168; intron 13 ABL1: 9: 133605893; intron 1b		b2a2
AZV-N-P102	GGTCAAGCTGTTTTGCATTCACTGTTGCACATATGCTCAGTCACACACACAGCATACGCTATGCACATGTGTCCACAGCACTTTGGGAGGCTGAGGTGAGTAGATCACTTGAGACCAGGAGTTCAAGACCAGCCTGGCCAACATGGCAAAACCCCGTCTCTACTGAAAATGAAAAAA	BCR: 22: 23632233; intron 13 ABL1: 9: 133723637; intron 1a		b2a2
AZV-N-P103	GCAAGACTCCGCCTCAAAAAAAAAAAAAAAAAAGTTCCTAGAAACAGCAAAATGTGGAGACAGAAAGCTTACCAGGGATTGTTGGGGAATACTCCCTTTCTTTTTTGACAGAGTCTCACTGTGTTG	BCR: 22: 23633468; intron 14 ABL1: 9: 133625843; intron 1b		b3a2
	TCTCATCGTAGGGGCTTTAGCTGGGGTTTGTGGATCGACTGAGTGAACGAATGTTGTGGGAAGTCCCGTTTCCCAGCCGCACCC	BCR: 22: 23634546; intron 14		b3a2

AZV-E-P104	AGGGAAATTCCACAGAGCGGGCAGGGGCATCTTTGTAAACATTTTTCATCAGTGACTCACAGCTTTGAGAAAGGATTATTTTTATATAAAACGA	ABL1: 9: 133722214; intron 1a		
AZV-N-P105	GTTAGCACTTTTGATGGGACTAGTGGACTTTGGTTCAGAAGGAAGAGCTATGCTTGTTAGGGCCTCTTGTCTCCTCCCAGGAGGGCAGGTGAATCGCTTGAACCCGGGAGGTGGAGGTTGCAATGATCCGGGATCGTGCCACTGCACTCCAGCCGGGGTGACAGAGTGAGACTC	BCR: 22: 23631969; intron 13 chr9:133584075; between EXOSC2 a ABL1	intergenic region	b2a2
AZV-E-P106	AAAGGGTCCCCACTACCAGGCCTCTCCATCCCCAGTCTCAGGTAGTTTTTCTAAAATGCAAACCCCACCCTGCAACTTACCGCCCACAGCGTGGCTAATCTTTGAAATTCTTGGCTGGGCTCGG	BCR: 22: 23634178; intron 14 ABL1: 9: 133599893; intron 1b		b3a2
AZV-I-P107	GGAATGGATGAATTACATGACATGCAGATTGCACCTTCATAACATAATCTTTCTCCTGGGCCCCTGTAGTAATCTCTTCCTCGTTGATGAAGCTTTCATCCTGTCTTCTCCCTGTTTAGA	BCR: 22: 23633667; intron 14 ABL1: 9: 133590447; intron 1b		b3a2
AZV-E-P109	GCTGACCAACTCGTGTGTGAAACTCCAGACTGTCCACAGCATTCCGCTGACCATCAATAAGGAAGGTGGGCCCCCCCGTTTCCGTGTACAGGGCACCCGATTGTCAGCCAGATAATTTTGTGAGAGAACAAAGCTAAACCAAATCACATCTGAATTTATAAATTCCAGTTCTAAATC	BCR: 22: 23631840; intron 13 chr9:133586088; between EXOSC2 a ABL1	intergenic region	b2a2
AZV-N-P110	GGATCGACTGAGTGAACGAATGTTGTGGGAAGTCCCGTTGTTGGTTGGGACTGAACTGTATTGCTGACCCTTTCCCAT	BCR: 22: 23634500; intron 14 ABL1: 9: 133639766; intron 1b		b3a2
AZV-N-P111	GCCAGGCTAGGCAGTGGGCACCTGTAATCACAACTGCTTGGGAGGCTGAGGGAAGAGAATCGCTTGAACCCAGGAGGCGGAGGTTGCAGTGAGCCGAGCTCCGAGCAGTAGATTACATTTGGATTTGAATGTAAGTGGCTGTGAATTCCAAATATTTGTTGGAATTATAAAGTGTC	BCR: 22: 23291161 ; intron 14 ABL1: 9: 130783464 ; intron 1		b3a2
AZV-S-P112	TCTATGGGTTTCTGAATGTCATCGACCACTCAGCCACTGGATTTAAGCAGAGTTCAAGTAAGTACTGGTTTGGGGAGGAGGGTTGCAGCGGCCGAGCCAGGGTCTCCACCCAGGAAGGACTAAACGAACTCTAGGGAGAGTAAATGGCACTTGTCACAGTGCAGTCAGGAGAGGC	BCR: 22: 23632664; intron 14 ABL1: 9: 133719120; intron 1a		b3a2
AZV-N-P114	TGTGCCACTGCATTCCAGCCTGGGCGACAGAGCAAGACTCCGCCTCAAAAAAAAAAAAAAAAAAAGTTCCTAGAAACAGCACACACACAATCAATCAAACATTCACAATGTGGTTATTAAAGGCTGTAATTAGGGGGACAATGAACCACAGGGATGGCTCAGAAGGTCAGAGCACTGAT	BCR: 22: 23633425; intron 14 ABL1: 9: 133615576; intron 1b		b3a2
AZV-N-P115	CTTCGAGTCACTGGTTTGCCTGTATTGTGAAACCAACTGGATCCTGAGATCCCCAAGACAGAAACACCTTTTTCTAACAACACGTACAGCACAGTCTTTCTGTGTTTGCAGCTTGGAACTGAGCAGCCCTC	BCR: 22: 23632361; intron 13 ABL1: 9: 133696048; intron 1b		b2a2
AZV-N-P116	TGCTGTCCTTGGAACCTTATTACACTTCGAGTCACTGGTTTGCCTGTATTGTGAAACCAACTGGATCCTGAGATCCCCAAGACAGAAATCATGACACATTACTATCTTGTTGAATTAAACGTTGCAAACTGCAACGTTTGTAACTGCCAGTAGGCAGTTTTTATTTTATTTTTCATTTTTT	BCR: 22: 23632360; intron 13 ABL1: 9: 133669609; intron 1b		b2a2
AZV-N-P117	GGGAAGTCCCGTTTCCCAGCCGCACCCAGGGAAATTCCACAGAGCGGGCAGGGGCATCGCATGAGGTGCTGGTGTTCACGCCAGACCACAATTAGGTGTTTAATTCGATTAGTTTCCCTTGTTTTTGTTTTTAATATTCCCTTGTTATCCTTTTAATGTCTATAGGGTCTGTGGTGAT	BCR: 22: 23634592; intron 14 ABL1: 9: 133601765; intron 1b		b3a2
AZV-E-P118	TGCATCCCCAAACCAAACCTATTATTCATGGACCCCAAACTTGTTCCTCTTATGTCCTGTCCCTTTGAGGGGCACCACCATCCACCCGCATGGCCAAGCCAGAAACCGTGGTCTGCTCTTTCCCCTTTTTTATTAGCAGTTTTACTGAGGTGTAATTTATATGCCATAAAATTTACCATT	BCR: 22: 23633972; intron 14 ABL1: 9: 133696189; intron 1b		b3a2
AZV-N-P119	GGTCCCCACTACCAGGCCTCTCCATCCCCAGTCTCAGGTAGTTTTTCTAAAATGCAAACCCCACCCTGCAACTTACCGCCCACACACACACAATCAATCAAACATTCACAATGTGGTTATTAAAGGCTGTAATTAGGGGGACAATGAACCACAGGGATGGCTCAGAAGGTCAGAG	BCR: 22: 23634174; intron 14 ABL1: 9: 133615574; intron 1b		b3a2
AZV-E-P120	CTGCCCGTGGTCCGGGCTTGTCTCTCCTTGCCTCCTGAGGTGCGGTGGCTCATGCCTGTAATCCCAGCACTTTGGGAGGCCAAGGCAGATGGATCACTTGAGCCCAGGAATTCAAGACCAGCCTGGGC	BCR: 22: 23633808; intron 14 ABL1: 9: 133596818; intron 1b		b3a2
AZV-E-P121	AGAGTTCAAGTAAGTACTGGTTTGGGGAGGAGGGTTGCAGCGGCCGAGCCAGGGTCTCCACCCAGGAAGGACTAATCGGGCAGGGTGTGGGGAAACAGGGAGGTTGTTCAAAATCTGATTTTCTGTTGCGTGTTCCTTGTAGCCATAGATGTGATTATGTCCACACCGGGCTGCCTTAATCTGTCCTGCTTGGAGAGTGACTTGTAAGATGCTGAATTATTCATGATAATACAGTG	BCR: 22: 23632701; intron 14 EXOSC2: 9: 133579956; exon 9	alternative splicing	b3a2

AZV-I-P122	ATCGGGCAGGGTGTGGGGAAACAGGGAGGTTGTTCAGATGACCACGGGACACAACTGGAGTTTTTATGTGCTGTTTTTGGCAG AGCCAAGTGAAGATCTTGTTACTTAGCCATTCCTGAGGTACTGAAGATACCCGGGTTTTTGTCATTACAGGATAGGCTAGAAAGT AGCCAGG	BCR: 22: 23632716; intron 14 ABL1: 9: 133709148; intron 1b		b3a2
AZV-E-P123	GGGAAGTCCCGTTTCCCAGCCGCACCCAGGGAAATTCCACAGAGCGGGCAGGGGCATCGCATGAGGTGCTGGTGTTCACGCCA GACCACAATTAGTTCATTCAGAAATACCCCAACATTGGGTGACTGCAGTCAACAAAGGCTTCTGTTGGATGAACTTGCATTTGAC AGCTGAA	BCR: 22: 23634583; intron 14 ABL1: 9: 133590783; intron 1b		b3a2
AZV-E-P124	TGGTGCTGTTTGCGCTCACATTTACATTTCCTAAAATTCTTTAAACCCTACACTTGGAATGGATGAATTACATGACATGGATTCAG TGCAGATGAAGTGCTGGCACTTGATACGGGATCAGTAAGTATTAGCTATTATTCTATCACATTAAGTTGCATAAACTTTAACCTCA TTACTCTTAA	BCR: 22: 23633623; intron 14 ABL1: 9: 133717682; intron 1a		b3a2
AZV-E-P125	ACATGAGTTGCACTGTGTAAGTTTCTCGAGGCCGGGCGCAGTGGCTCATGCCTGTAATCCCAGCACTTTGGGAGGCTGAGGCAG GTGGATCGCTTGAGCTCAGGAGTTGGAGACCAGCCTGACCACACCCTTCTACATCTTTCTGTCTGGATGAAGCTCCTCTGCTGTC ATTTCCT	BCR: 22: 23633208; intron 14 ABL1: 9: 133662030; intron 1a		b3a2
AZV-N-P127	TTTTTTCCTTTCCCTCTAAGTGGGGGTCTCCCCCAGCTACTGGAGCTGTCANAACAGTGAAGGCTGGTAACACATGAGTTGCACT GTGTAAGTTTCTCGAGGCCGGGCGCAGTGGCTCATGCCTGTAATCCCAGCACTTTGGGAGGCTGAGGCAGGTGGATCGCTTGA GCTCAGGAGGCAAAATGATTANCTTTAACAGTAGGATTAATTTTTTTTAAATGTATATAAAAATACTTGTATGTAANAAATCCTA	BCR: 22: 23633188; intron 14 ABL1: 9: 133713772; intron 1a		b3a2
AZV-N-P129	GGGTGCCCGGGAGTGTTGGGTCCAAGCCAGGAGGGCTGTCAGCAGTGCACCTTCACCCCACAGCAGAGCAGATTTGGCTGCTC TGTCGAGCTGGATGGATACTACTTTTTTTTTCCTTTCCCTCTAAGTGGGGGTCTCCCCCAGCTACTGGAGCTGTCAGAACAGTGAA GGCTGGTAACACATGAGTTGCACTGTGTAAGTTTCTCGAGGCCGGGCGCAGTGGCTCATGCCTGTAATCCCAGCACTTTGGGAG	BCR: 22: 23633165; intron 14 ASIC2: 17: 32073433; intron 1 ABL1: 9: 133600059; intron 1b	fusion BCR/ASIC2/ABL1	b3a2
AZV-N-P130	TTGCACATATGCTCAGTCACACACACAGCATACGCTATGCACATGTGTCCACACACACCCCACCCACATCCCACATCACCCCGACC CCCTCTGCTGTCCAAACCCAGCCTTAATTTGCTCTTCTTTGATGACTCATGAGGTTAAGCACCTTTTCATATGTTTACTGGCCATTT GGAATA	BCR: 22: 23632281; intron 13 ABL1: 9: 133605781; intron 1b		b2a2
AZV-E-P131	CCCAGCCCTCCTCTCCTCCAGCTACCTGCCAGCCGGCTTCTCTTATGTAACTATAGTATAATTATTAACTTTAGGAAATTTAACTTT GATAGAATATTTTTATTTAACCTAAAATCCGTATTCCAATTTCCTCAATTCTCCCAGTAATGTCCTTTCTAGCAATTACCCCCTTGGG TGTAGG	BCR: 22: 23632151; intron 13 ABL1: 9: 133663835; intron 1b		b2a2
AZV-E-P132	ATGCACATGTGTCCACACACACCCCACCCACATCCCACATCACCCCGACCCCCTCTGCTGTCCTTGGAACCTTGGAAATTGGCTAT ATACTCACGATAGCCAAGAACAAGAACACTCTCTTACACCATCACATCATTGCCACACTTAAGGAAATCCACACTGATCCAGGAA CATTATT	BCR: 22: 23632288; intron 13 ABL1: 9: 133658365; intron 1b		b2a2
AZV-S-133	AAAAAGTTCCTAGAAACAGCAAAATGTGGAGACAGAAAGCTTACCAGGGATTGTTGGGGAATGGGGTTGTTGTCCCCCTGATC ATTACTGATTGAAACAAGAAATCTGTTGTTCCTGGATTTCTTTCAGTTATCTTAACATAGACCCTTCCAAGTCTTACAGATGTCAA GGGTTTTTGAA	BCR: 22: 23633475; intron 14 ABL1: 9: 133635754; intron 1b		b3a2
AZV-N-B134	GATGTGGAAAANACCTGTGACCTTCTCCATGTCCTCTTCTCCCCACANATCTGTACTGCACCCTGGAGGTGGATTCCTTTGGGTAT TTTGTGAATAAAGCAAANACNCNCGTCTACAGAGATTATTAACTCAGTTTATTATC	BCR: 22: 23634797; exon 15 ABL1: 9: 133679187; intron 1b	non-complete exon 15	b3a2
AZV-N-B135	AACTCCAGACTGTCCACAGCATTCCGCTGACCATCAATAAGGAAGGTGGGCAGGTTAACAAGTCCTGCACTAAGGAATTGGCTC AGTAAAACCTCAGCATTCTCACAGGAAGAGCCTA	BCR: 22: 23631813; intron 13 ABL1: 9: 133720387; intron 1a		b2a2
AZV-N-B136	CCCTCTGCTGTCCTTGGAACCTTATTACACTTCGAGTCACTGGTTTGCCTGTATTGTGAAACCAACTGGATCCTGAGATCCCCAAG ACTTTCCTGCATTTTTGCATGTTAAATAATTTTGATTGTATGCCANACATGTGGGTGTTATNNNGTAGGGATTCTCAATCTTTGTT ATCTTTCTT	BCR: 22: 23632356; intron 13 ABL1: 9: 133604263; intron 1b		b2a2
AZV-S-B137	TTACAGACCATGTGGGTGATGTGGAAAAGACCTGTGACCTTCTCCATGTCCAGTAAAACAAAAATATCTGTTTATTTGTGTATGT CCAGGAAAAAAAAGTATGGAAGGATTTTACACCGAAATTTTTATCTCTAGGGACTTGGAGCT	BCR: 22: 23634714; intron 14 ABL1: 9: 133594424; intron 1b		b3a2
AZV-N-B138	TCTTTGGTCTCTTGCGCAGATGATGAGTCTCCGGGGCTCTATGGGTTTCTGAATGTCATCGTCCACTCAGCCAAAATATATATTTA TTACACAAAAGATAGCATACAGTATATACCGTTCTGTACCTTCTTTTTTGTTTTTCCCTTAATAGATCCTCAGGATCTCCCCATATTG GAATATG	BCR: 22: 23632580; exon 14 ABL1: 9: 133610910; intron 1b	non-complete exon 14	b2a2
AZV-N-B139	GGCTTGTCTCTCCTTGCCTCCCTGTTACCTTTCTTTCTATCTCTTCCTTGCCCCGTGCACTCAACCTTGCATCCCCAAACCAAACCTA TTATTCATGGACCCCAAACTTGTTCCTCTTATGTCCTGTGTGAGATAACTACTCTTATGACTACCTCCCATTTTTCAGATGAGAAAA	BCR: 22: 23633913; intron 14 ABL1: 9: 133706157; intron 1b		b3a2

	TTGAG			
AZV-N-B140	TTCCCGGAGTGGCCTCTGCCCTCTCCCCTAGCCTGTCTCAGATCCTGGGAGCTGGTGAGCTGCCCCCTGCAGGTGGATCGAGTAA TTGCAGGGGTTTGGCAAGGACTTTCTCAATTGTTTTCCATTTTATTGATTTCTGCTCTTTATTTTCTTTCTTTTACTTAAAAAAANTT TTTTTT	BCR: 22: 23632884; intron 14 ABL1: 9: 133601967; intron 1b		b3a2
AZV-N-B141	CCTCCTCCCTGGTCTTTGTAGCTCTGGATATCCTGAACACGTGACATTATGTAGCAAGTCTCTGAGTCTGTTCATTTTTTTCCTTCA GTCTTTTTTTTTTTTTTTGAAATGGTCTCTCTCTGTTGCCCAGGCTG	BCR: 22: 23634082; intron 14 ABL1: 9: 133677427; intron 1b		b3a2
AZV-N-B142	TGTTGGGGATGGGGCTGGGAGAGAGGACTAACTGCAGATGAACCCAAGGGGGACTTTTTAGGTGAGAGCAGTGTCGTGAAAA GACTGTGGTGCTGTTTGCGCTCACATTTACATTTCCTAAAATTTTAGAGACAGAGTCTTGCTTTGTCACCCAGGCTGGAGTGTAGT GGCACAGT	BCR: 22: 23633580; intron 14 ABL1: 9: 133597889; intron 1b		b3a2
AZV-N-B143	AACCCTCCTCCCCAAACCAGTACTTACTTGAACTCTGCTTAAATCCAGTGGCTGAATAGTCTTTGTTGAAGGAACGAATTAGTGCA TCCTTCCAAGCCTTGGAGGACCTGTCTATAATAG	BCR: 22: inversion ABL1: 9: 133644046; intron 1b		b2a2
AZV-N-B144	GTGGCATCACTGTGTAACAATGGCGTGTACACCTCTCTGTCCCCACCAGTGCAGGGCCCTTCTCATCGTAGGGGCTTTAGCTGGG GTTTGTGGATCGACTGAGTGAACCAGTGTTGAAATCTGACATTTTTTTAATCTCATGAACTCCACAATTGTCTGATTATTAAAGTC CTGCTTACTTGACTGTGACTAAAATTCTACTTTCAGAAGAGTAGAATGTACCCCTACCAAATTGAAG	BCR: 22: 23634479; intron 14 ABL1: 9: 133621103; intron 1b		b3a2
AZV-N-B145	CGCAGTGGCTCATGCCTGTAATCCCAGCACTTTGGGAGGCTGAGGCAGGTGGATCGCTTGAGCTCAGGAGTTGGAGACCAGCC TGACCAACATGGTGAAACAGGGTGAATAAACCTTCTACAATCACAGGCCTAGAAAGTTTTTCTTTTTCTTACGGAATTTCTTGACT GTTTACTTGTACTANATATTTCTTCGGTATATTCATAATGACAGAACAATTGTTTATGATTGATTGATC	BCR: 22: 23633220; intron 14 ABL1: 9: 133680798; intron 1b		b3a2
AZV-N-B146	GGGAAATTCCACAGAGCGGGCAGGGGCATCGCATGAGGTGCTGGTGTTCACGCCAGACCACAATTAGGTGTTTAATTTTTAAAA AGAAAGTTACAACCTTTTTTTTTTATTTTTATTTTTTCTGAGATTTTTCAGTTTATTTCTTCTAAGTTTTGTCAGTTGAACAGTAGGG ATAAATTAA	BCR: 22: 23634641; intron 14 ABL1: 9: 133625676; intron 1b		b3a2
AZV-N-B148	AGGAAGAGCTATGCTTGTTAGGGCCTCTTGTCTCCTCCCAGGAGTGGACAAGGTGGGTTAGGAGCAGTTTCTCCCTGAGTGGCT GCTGCTGGGTGGTTGAGGAGATGGAACCCGGGAGGCGGAGCTTGCAGTGGGCGGAGATCGCGCCACTGCACTCCCGCCTGGG TGACAGAGCGAGACTACGTCTCAAAAAAAAAAAAAAAAAAAA	BCR: 22: 23632032; intron 13 ABL1: 9: 133704871; intron 1b		b2a2
AZV-N-B149	ATGCACATGTGTCCACACACACCCCACCCACATCCCACATCACCCCGACCCCCTCTGCTGTCCTTGGAACCTTATTACACTTCGAG TCACGTCCAGTGGCACAGTCTCGGCTCACTCCAACCTTGACCTCCTGGGCTCAAGCGGTCCTCCAACTTCATCCTCCTGAGTAGCT GGGAC	BCR: 22: 23632308; intron 13 ABL1: 9: 133605010; intron 1b		b2a2
AZV-N-B150	TAAGGAAGGTGGGCCCCCCCGTTTCCGTGTACAGGGCACCTGCAGGGAGGGCAGGCAGCTAGCCTGAAGGCTGATCCCCCCTT CCAGGAGTTCGAGACCAGCCTGGCCAACGTTCGAGACCAGCCTGGCCAACATAGTGAAACCCTGTCTCTATTAAAAATACAAAA ATTAGCTGAGCGTGGTGGCACATGCCTGTAGTCCCAGCTACTCGGGAG	BCR: 22: 23631885; intron 13 ABL1: duplication		b2a2
AZV-N-B151	AGGACTAATCGGGCAGGGTGTGGGGAAACAGGGAGGTTGTTCAGATGACCACGGGACACCTTTGACCCTGGCCGCTGTGGAG TGTTTGTGCTGGTTGATCCTGAGGATGTTGGGAAGGACAGATTGTACTTACCAAGAGCATTTATTGTTGTTTTTATTTTCTTAAAC ATTTCCAATGAAAATCATCAAACCTATAAAGTTGAAAGAACAATGCACCTAGATTCATCAACTCTTAAC	BCR: 22: 23632757; intron 14 ABL1: 9: 133658181; intron 1b		b3a2
AZV-N-B152	AGGTGGGTTAGGAGCAGTTTCTCCCTGAGTGGCTGCTGCTGGGTGGTTGAGGAGATGCACGGCTTCTGTTCCTAGTCACAAGGC TGCAGCAGACGCTCCTCAGATGCTCTGTATCCGGAGTTTATATTTCTTGAAAAGCTCATTACAGGTAGTTGCTGGAATGAGATAG TTTGTGTG	BCR: 22: 23632087; intron 13 ABL1: 9: 133613799; intron 1b		b2a2
AZV-N-B153	ATGCACATGTGTCCACACACACCCCACCCACATCCCACATCACCCCGACCCCCTCTGCTGTCCTTGGAACCTTGGGATTGGTGAGT GCCACAGCTTCCTGCCCCTTAACAGATCAGTG	BCR: 22: 23632289; intron 13 ABL1: 9: 133617295; intron 1b		b2a2
AZV-S-B154	TCAGTCACACACACAGCATACGCTATGCACATGTGTCCACACACACCCCACCCACATCCCACATCACCCCGACCCCCTCTGCTGTC CTTGGAACCTTATTACACTTCGAGTCACTGGTTTGCCTGTATCACAGGGTTTCACCATGTTAGTCAGGCTGGTCTCGAACTCCTGA CCTCAGGTGATCTGCCCCTCAGCCTCCCAAAGTGCTGGGATTCCAGGT	BCR: 22: 23632326; intron 13 ABL1: 9: 133626224; intron 1b		b2a2
AZV-N-B155	TTCGAGTCACTGGTTTGCCTGTATTGTGAAACCAACTGGATCCTGAGATCCCCAAGACAGAAATCATGATGAGTATGTTTTTGGC CCATGACACTGGCTTACCTTGTGCCAGGAGAGCCAATGATGTGGCTATAGTCCAAAGGCTGACAGGCTCAAGACCCAGGCAGA GCCAATGTTTCAGTTCAAGTCCAAAGGCAGGAAAAAAGTTGATGTCCCAGTTCGAAGGCAGTTAGGC	BCR: 22: 23632408; intron 13 ABL1: 9: 133684928; intron 1b		b2a2
	GCAGGTGGATCGCTTGAGCTCAGGAGTTGGAGACCAGCCTGACCAACATGGTGAAACCGGGCTGCCTTAATCTGTCCTGCTTGG	BCR: 22: 23633218; intron 14	alternative splicing	b3a2

AZV-N-B156	GCAGGTGGATCGCTTGAGCTCAGGAGTTGGAGACCAGCCTGACCAACATGGTGAAACCCCGCTCTCTAAAAATACAAAAATTAGCCGGGCGTGGTGGCGCGCGCCTGTAATCCCAGCTACTCGGGAGGCTGAGGCAGGAGAATCGCTTGAACCCGGGAGGCGGAGGTTGCAGTGAGCCGAGATCGCGCCACTGCACTCCAGCCTGGGCGACAGAGTGACTTGTAAGATGCT	EXOSC2: 9: 133580008; exon 9		
AZV-N-B157	GGTCAAGCTGTTTTGCATTCACTGTTGCACATATGCTCAGTCACACACAGCATACGCTATGCACATGTGTCCACACACACCCCACCCACATCCCACATCACCCCGACCCCCTCTGCTGTCCTTGGAGCCAGGCGTAGTGGGGAGTGCCTGTAATCCCAGCTACTCAGGAGGCTAAGGCAGGAGAATTACTTGAACCTGGGAGGCAGAGGTTGCAGTGAGCCGCGATCTCACCA	BCR: 22: 23632285; intron 13 ABL1: 9: 133717052; intron 1a		b2a2
AZV-S-B158	AGCATACGCTATGCACATGTGTCCACACACACCCCACCCACATCCCACGTCACCCCGACCCCCTCTGCTGTCCTTGGAACCTTATTACACTTCGAGTCACTGGTTTGCCAGTGGCATTAAGTATATTCCCAGTGATGCAGTCATCATCACTATCCATTTTCAGAACTTTTTCATCATCCTAAGTAGAAACTCTGTACCCATTAAAAAATAATATNNNNNTTC	BCR: 22: 23632316; intron 13 ABL1: 9: 133600516; intron 1b		b2a2
AZV-N-B160	TGTTGGGGATGGGGCTGGGAGAGAGGACTAACTGCAGATGAACCCTATTTACTACCAAATAATCTTTTTAAATGAAAAATTTGTTATCCCTCCCAGCCCTCAGCCATGACCCGAAGTA	BCR: 22: 23633503; intron 14 ABL1: 9: 133624308; intron 1b		b3a2
AZV-N-B161	GATGCTCTGTGCCTTGGATCTGGCCCCACTCCCGTCCTCCCAGCCCTCCTCTCCTCCAGCTACCTGCCAGCCGGCACTTTGGTCGGGAGCCTGATCCTTGGAGCCAGGCAGACCTGGGTTGAGTCCATCTCCGCCTGTTTCCAG	BCR: 22: 23632156; intron 13 ABL1: 9: 133709393; intron 1b		b2a2
AZV-S-B162	AGCAGTGTCGTGAAAAGACTGTGGTGCTGTTTGCGCTCACATTTACATTTCCTAAAATTCTTTAAACCCTACACTTGGAATGCAGTGCGCGATCTCCGCTCACTGCAAGCTCTGCCTCCCGGGTTCATGCCATTCTCCCGCCTCAGCCTCCCAAGTACTGGGACTACAGGCACCCA	BCR: 22: 23633599; intron 14 ABL1: 9: 133697275; intron 1b		b3a2
AZV-N-B163	CTGGGTGGTTGAGGAGATGCACGGCTTCTGTTCCTAGTCACAAGGCTGTGAGCCAAGATTGCACCACTGCACTCCAGTCTGGGCAACAAGAGTGGGACTCTGTCTC	BCR: 22: 23632061; intron 13 ABL1: 9: 133629536; intron 1b		b2a2
AZV-N-B164	GGGAGAGAGGACTAACTGCAGATGAACCCAAGGGGGGACTTTTTAGGTGAGAGCAGTGTCGTGAAAAGACTGTGGTGCTGTTTGTTCAGTGTACTCTCATGGCAAAACTGCTGGTGAGTGTACCCTTTCTGCAGAAAGTAAAAAATGGCCTTGCTGAGGAAATTAAATTTATGTTCA	BCR: 22: 23633553; intron 14 ABL1: 9: 133692989; intron 1b		b3a2
AZV-N-B165	GGNAGGCAGCTAGCCTGAAGGCTGATCCCCCCTTCCTGTTAGCACTTTTGATGGGACTAGTGGACTTTGGTTCAGAAGGAAGTTTTTAAATGAAAAGATCAACAAATCCAAATGCTGTGGTATTTATACTGATTTAGAAAGGCAGTTGACTTTGGGAGGCTTTGTTTTCTCATTTCCCTT	BCR: 22: 23631931; intron 13 ABL1: 9: 133631511; intron 1b		b2a2
AZV-N-B166	ACTGGCTTACCTTGTGCCAGGCAGATGGCAGCCACACAGTGTCCACCGGATGGTTGATTTTGAAGCAGAGTTAGCTTGTCACCTGCCTCCCTTTCCCGGGACAACAGAAGCTGACCTCTTTGATCTCTTGCGCAGATGATGAGTCTCCGGGGCTCTATGGGTTTCTGAATGTCATCGTCCACTCAGCCACTGGATTTAAGCAGAGTTCAAGTAAGATCAATTCAGCATGCATGTATGGGTCACTTGTATGTTTTT	BCR: 22: 23632602; intron 14 ABL1: 9: 133694157; intron 1b		b3a2
AZV-N-B170	TCTGTACTGCACCCTGGAGGTGGATTCCTTTGGGTATTTTGTGAATAAAGCAAAGACGCGCGTCTACAGGGACAATCTCAGCTCATTGCAACCTCCACCTCCCGAGTTCAAGCGATTCTCTTTCCTGCCTCAGCCTAATTTTTTGTATTTTTATTAAAGACGG	BCR: 22: 23634799; exon 15 ABL1: 9: 133597270; intron 1b	non-complete exon 15	b3a2
AZV-N-B171	GAGGGAAGAGAATCGCTTGAACCCAGGAGGCGGAGGTTGCAGTGAGCCGAGCTTGTTTCTTGTTTCCATTCTTTTCTTACCATATGACCAAGTAAGTCCAAGAAAGTAGATAGGATTCTGAGTGGGCA	BCR: 22: 23633367; intron 14 ABL1: 9: 133656117; intron 1b		b3a2
AZV-N-B172	TCTCTGGCTGCCTCATAAACGCTGGTGTTTCCCTCGTGGGCCTCCCTGCATCCCTGCATCTCCTCCCGGGTCCTGTCTGTGCCAGCCTGGGCGACAGAGCGAGACTCCGTCTCAAAAAAAAAAAAAAAAAAAAAAAATTTACTATCATGTAAAGGGGAGTTGGTCTCACCCTACACTG	BCR: 22: 23633747; intron 14 ABL1: 9: 133629863; intron 1b		b3a2
AZV-N-B173	GCATGAGGTGCTGGTGTTCACGCCAGACCACAATTAGGTGTTAGAATATTTTTATTTAACCTAAAATCCGTATTCCAATTTCCTCAATTCTCCCAGTAATGTCCTTTCTAGCAATTACCC	BCR: 22: 23634587; intron 14 ABL1: 9: 133663888; intron 1b		b3a2
AZV-N-B174	GTAAGTACTGGTTTGGGGAGGAGGGTTGCAGCGGCCGAGCCAGGGTCTCCACCCAGGAAGGACTCATCGGGCAGGAGCAAGAATGAATTGTTTAATATTAAAAACATTATAGCCCAAATTTAAAATCCAACAGAAGATGTGGAAAATTGTCTCAGAATGTATTGGGTTGGTACAAAA	BCR: 22: 23632675; intron 14 ABL1: 9: 133703751; intron 1b		b3a2
AZV-S-B175	CTCATGCCTGTAATCCCAGCACTTTGGGAGGCTGAGGCAGGTGGATCGCTTGAGCTCAGGAGTTGGAGACCAGCCTGACCAACAGGCAGGCCTGCCTCCAAGATGGNTCNNTCACAGGGCTGGCGAGCAGTGCTGGCAGTTGACAGGAGGCCACAGTTCCTTGCCACACGGA	BCR: 22: 23633211; intron 14 ABL1: 9: 133638963; intron 1b		b3a2

AZV-N-B175	CAGAAGCTGACCTCTTTGATCTCTTGCGCAGATGATGAGTCTCCGGGGCTCTATGGGTTTCTGAATGTCATCGTCCACTCAGCCA CTGGATTTGAGCAAGGTTTAAATATTTCCCCTGGAATCTTTTACATGACAATGTCTTAGCCAGACAATTTTTAAGAAACAAAATTC TCCATCCTAACTCCTATCCCCATCAACAGTCCAAATCTTAACCTTTCTTTTTTTTTTT	BCR: 22: 23632590; exon 14 ABL1: 9: 133720613; intron 1a	non-complete exon 14	b2a2
AZV-S-B176	TGGGAGAGAGGACTAACTGCAGATGAACCCAAGGGGGACTTTTTAGGTGAGAGCAGTGTCGTGAAAAGACTGTGGTGCTGTTT GCGCTCACATTTACATTTCCTAAAATTCTGAGCCTGAAGAAAGGCAGAGGACACCAGTAGGCATCTTGGATGTGGGATTGGTCA GAGGGGAGAGAGGTAAAAATGATTCCATGACTGTGAGTCTGGCGACTAGAAATGGGGGTGACATTCAC	BCR: 22: 23633585; intron 14 ABL1: 9: 133630629; intron 1b		b3a2

Table S4. The likelihood for prediction of TFR. The chi-square tests follow whether there is a significant difference between the Log-likelihoods (specifically the -2LLs) of the baseline model and the new model. If the new model has a significantly reduced -2LL compared to the baseline then it suggests that the new model is explaining more of the variance in the outcome and is an improvement. Here the chi-square is highly significant for the model BCR-ABL1 DNA+/- and RNA+/- compared to other two models.

DNA and RNA pattern during DMR mantenance before TKI stop/interruption	**-2 Log Likelihood**	**Chi-square**	**P value**
Model BCR-ABL1 RNA+/-	133.69	10.49	0.001
Model BCR-ABL1 DNA+/-	132.63	11.49	0.001
Model BCR-ABL1 DNA+/- and RNA+/-	128.25	15.92	0.000

Table S5 Sensitivity, specificity, PPV and NPV of the traffic light model

A.	**MRFS**	**Mol. Rel.**	**Sensitivity**	**Specificity**	**PPV**	**NPV**
Green	10	1	0.48	0.95	0.91	0.65
Yellow+Red	11	20				
B.						
Green+Yellow	18	9	0.86	0.57	0.67	0.80
Red	3	12				

Mol. Rel. – molecular relapse (loss of MMR); MRFS – molecular relapse-free survival, PPV – positive predictive value, NPV – negative predictive value